An analytical platform for the screening and identification of pyrrolizidine alkaloids in food matrices with high risk of contamination

Food Chemistry

An analytical platform for the screening and identification of pyrrolizidine alkaloids in food matrices with high risk of contamination

--Manuscript Draft--

Manuscript Number:	FOODCHEM-D-22-06697R1
Article Type:	Research Article (max 7,500 words)
Keywords:	Bee products; Dietary supplements; Herbal products; Spectral library; Suspect screening; Target screening
Corresponding Author:	anna lisa piccinelli, Prof University of Salerno Department of Pharmacy Fisciano, salerno ITALY
First Author:	Serena Rizzo, Dr
Order of Authors:	Serena Rizzo, Dr
	Rita Celano, PhD
	Anna Lisa Piccinelli, Prof
	Simona Serio
	Mariateresa Russo
	Luca Rastrelli
Abstract:	An analytical platform for the detection of pyrrolizidine alkaloids (PAs) in honey, pollen, teas, herbal infusions, and dietary supplements is proposed; it includes a wide-scope suspect screening method, based on a diagnostic product ion filtering strategy for the characterization of PAs, and a target screening and identification method for the high-throughput detection of 118 PAs of a high-resolution mass spectral library. Salting-out assisted liquid-liquid extraction of aqueous extracts combined to ultra-high performance liquid chromatography–high-resolution tandem mass spectrometry was employed. The limit of identification (0.6-30 μg kg–1) of 28 standards were fit-for-purpose in PA-monitoring applications, with a false negative rate < 1.3% at 4 μg L–1. The wide-scope suspect screening method allowed the tentative identification of 88 compounds. The screening of 282 commercial samples revealed a broad contamination of the studied matrices, demonstrating the effectiveness of the platform in detecting and identifying both target and untarget PAs.
Suggested Reviewers:	Natalia Casado Rey Juan Carlos University natalia.casado@urjc.es She has expertise in analysis of pyrrolizidine alkaloids
	Patrick P.J. Mulder Wageningen University & Research patrick.mulder@wur.nl He has expertise in analytical method for pyrrolizidine alkaloid analysis
	Jean-Francois Picron Sciensano Jean-Francois.Picron@sciensano.be He has expertise in determination of pyrrolizidine alkaloids in food matrices
	Alberto Angioni University of Cagliari aangioni@unica.it He has expertise in food safety
	Judith Mueller-Maatsch PhD, Wageningen University & Research judith.mueller-maatsch@wur.nl She has expertise in food safety and authenticity

An analytical platform for the screening and identification of pyrrolizidine alkaloids in food matrices with high risk of contamination

Serena Rizzo[1,2], Rita Celano[1], Anna Lisa Piccinelli[1]*, Simona Serio[1], Mariateresa Russo[3], Luca Rastrelli[1]

[1]Department of Pharmacy, University of Salerno, Via Giovanni Paolo II 132, 84084 Fisciano, Salerno, Italy

[2]PhD Program in Drug Discovery and Development, University of Salerno, Via Giovanni Paolo II 132, Fisciano, SA, 84084, Italy

[3]Department of Agriculture Science, Food Chemistry, Safety and Sensoromic Laboratory, University of Reggio Calabria, Via Salita Melissari, 89124, Reggio Calabria, Italy

*_Corresponding author at:_ Department of Pharmacy, University of Salerno, Via Giovanni Paolo II 132, 84084 Fisciano, Salerno, Italy

Tel.: +39(0)089969794

E-mail address: apiccinelli@unisa.it

Abstract

An analytical platform for the detection of pyrrolizidine alkaloids (PAs) in honey, pollen, teas, herbal infusions, and dietary supplements is proposed; it includes a wide-scope suspect screening method, based on a diagnostic product ion filtering strategy for the characterization of PAs, and a target screening and identification method for the high-throughput detection of 118 PAs of a high-resolution mass spectral library. Salting-out assisted liquid-liquid extraction of aqueous extracts combined to ultra-high performance liquid chromatography–high-resolution tandem mass spectrometry was employed. The limit of identification (0.6-30 μg kg^{-1}) of 28 standards were fit-for-purpose in PA-monitoring applications, with a false negative rate < 1.3% at 4 μg L^{-1}. The wide-scope suspect screening method allowed the tentative identification of 88 compounds. The screening of 282 commercial samples revealed a broad contamination of the studied matrices, demonstrating the effectiveness of the platform in detecting and identifying both target and untarget PAs.

Keywords: Bee products; Dietary supplements; Herbal products; Spectral library; Suspect screening; Target screening

1. Introduction

Pyrrolizidine alkaloids (PAs) are natural toxins produced by different plants (*Boraginaceae*, *Asteraceae* and *Fabaceae* families) as defense against insects and herbivores. The structures of PAs consist of the 1-hydroxymethyl pyrrolizidine core (necine base) esterified with one or two aliphatic acids (necic acids). PAs occur in plants as tertiary amines or N-oxide derivatives (PANOs) (EFSA, 2011; Moreira, Pereira, Valentão, & Andrade, 2018; Schramm, Köhler, & Rozhon, 2019).

Because of their wide distribution in plants and their high incidence of contamination in foods and herbal products, PAs are considered some of the most dangerous classes of phytotoxins in causing liver damage (Schrenk et al., 2020). In fact, PAs exhibit carcinogenic and genotoxic activities under chronic exposure and hepatotoxic activity as result of acute toxicity. In particular, PAs/PANOs containing a 1,2-unsaturated necine base are considered of higher toxicity due to their metabolic activation into dehydro-pyrrolizidine esters, which can readily react with proteins and form DNA adducts (Dusemund et al., 2018; EFSA, 2011; Schrenk et al., 2020).

Beside the intake of PAs through herbal products containing PA-producing plants (Steinhoff, 2019), in the last decades, numerous scientific reports have revealed a worrying contamination of PAs from food products of plant origin (such as beehive and herbal products), mainly due to their accidental contamination with PA-producing plants during harvest. The high number of PA-producing plants, their global occurrence and wide distribution as weeds in the agricultural areas (*Crotalaria spp.*, *Echium spp.*, *Heliotropium spp.*, *Myosotis spp.*, and *Senecio spp.*) make the contamination of PAs a relevant issue for the food safety and quality of herbal products (EFSA, 2016; Schrenk et al., 2020; Steinhoff, 2019). In particular, the chronic toxicity due to long-term consumption of PA-contaminated food or herbal medicines is a current topic for the human health.

The European Food Safety Authority (EFSA), in its recent risk assessments, recognized PAs as undesirable substances in food and concluded that there is a possible human health concern related to chronic cumulative exposure to contaminated food products, such as teas, herbal infusions, beehive products and dietary supplements (EFSA, 2011; EFSA 2016; EFSA, 2017). In addition, the European

Commission has recently established maximum levels (MLs) for the sum of 21 PAs and 14 of their co-eluting isomers in certain food products, which are teas, herbal infusions, dried herbs, pollen, dietary supplements containing herbal ingredients and pollen (European Commission, 2020). To reduce the chronic exposure to PAs, both the implementation of measures to mitigate their contamination and the development of new sensitive analytical procedures to evaluate their dietary exposure and collect occurrence data are important aspects to consider (EFSA, 2016; EFSA 2017).

Currently available methods for the sensitive determination of PAs in various matrices are based on solid phase extraction (SPE) followed by liquid chromatography coupled to tandem mass spectrometry (LC-MS/MS) with unit resolution spectrometric analyzers (triple quadrupole and ion trap). Selected reaction monitoring (SRM), also called multiple reaction monitoring (MRM), is a well-established MS/MS acquisition mode for the targeted analysis of PAs, due to its high selectivity, sensitivity, and robustness (Casado, Morante-Zarcero, & Sierra, 2022; Ma et al., 2018; Mulder et al., 2018; Picron, Herman, Van Hoeck, & Goscinny, 2018). Although it ensures excellent analytical performance, which easily meet the quality criteria required in food safety control, this approach presents limitations on the number of compounds to be analyzed in one run, requires the availability of reference standards, and it does not provide suitable MS/MS spectra for the screening and structural elucidation of unknown or suspected compounds (Hird, Lau, Schuhmacher, & Krska, 2014; Righetti, Paglia, Galaverna, & Dall'Asta, 2016).

In recent years, high resolution mass spectrometry (HRMS) has been increasingly used as complementary method for the analysis of trace-level contaminants in food matrices since it allows the simultaneous screening of target, suspect, and untarget compounds. Moreover, the acquisition of accurate MS and MS/MS spectra (resolution < 5 ppm) offers the possibility to detect a theoretically unlimited number of molecules without the need of a compound-specific tune, carry out the retrospective data analysis, and perform structural characterization of unknown or suspected compounds (Hird et al., 2014; Menger, Gago-Ferrero, Wiberg, & Ahrens, 2020; Rajski, Petromelidou, Díaz-Galiano, Ferrer, & Fernández-Alba, 2021; Righetti et al., 2016).

The analysis of PAs is a challenging task as the high variety of both necine bases and necic acids results in a huge number of different structures and numerous stereoisomers; to date, well over 600 PAs are known (Moreira et al., 2018; Schramm et al., 2019). The regulated list of PAs and PANOs to monitor is limited and the development of advanced analytical approaches to detect further PAs, which can potentially contaminate plant-based matrices, is of huge importance to better understand the presence of these contaminants in food matrices and guarantee their safety (Casado et al., 2022). This study aims to develop an analytical platform for the rapid and automated screening and identification of a high number of PAs and PANOs at trace levels in various food matrices to broaden the knowledge about the distribution of these contaminants in foods. To achieve this goal, an analytical procedure combining the salting-out assisted liquid-liquid extraction (SALLE) of aqueous extracts with ultra-high performance liquid chromatography coupled with high resolution tandem mass spectrometry (UHPLC-HRMS/MS) was established. A systematic workflow, based on a database (778 molecules) and a diagnostic product ion filtering strategy, was designed to first characterize PAs and PANOs from PA-producing plants and then create an in-house HRMS/MS spectral library. Furthermore, two software-assisted processing methods were implemented to automate and facilitate the detection and characterization of PAs and PANOs (wide-scope suspect screening method) and perform the rapid and reliable screening of 118 target PAs and PANOs in commercial samples (high-throughput target screening and identification method). The proposed platform was validated for six food matrices according to the European guidelines for qualitative screening methods (Magnusson & Örnemark, 2014; Pihlstrom et al., 2018). Finally, 282 commercial samples were screened to test the applicability of the screening and identification method and investigate the contamination profile of the food matrices of interest: honey, pollen, black and green teas, herbal infusions, and dietary supplements.

To the best of our knowledge, this is the first study which proposes an HRMS-based approach for the target screening analysis of a high number of PAs and PANOs and offers the possibility to detect and identify new targets of such a vast class of natural toxins.

2. Material and methods

2.1. Chemicals and standards

Analytical grade acetonitrile (MeCN), methanol (MeOH), magnesium sulfate heptahydrate ($MgSO_4 \cdot 7H_2O$), sodium sulfate (Na_2SO_4), sodium hydroxide (NaOH), sulfuric acid (H_2SO_4) and MS grade formic acid (HCOOH) were purchased from Merck Chemicals (Milan, Italy). MS grade MeCN and water (H_2O) were provided by Romil (Cambridge, UK). Ultrapure water (18 MΩ) was prepared using a Milli-Q purification system (Millipore, Bedford, USA).

Reference standards (n = 30) (85-98 % HPLC grade) of echimidine, echimidine N-oxide, erucifoline, erucifoline N-oxide, europine, europine N-oxide, heliotrine, heliotrine N-oxide, indicine, indicine N-oxide, intermedine, intermedine N-oxide, jacobine, jacobine N-oxide, lasiocarpine, lasiocarpine N-oxide, lycopsamine, lycopsamine N-oxide, monocrotaline, monocrotaline N-oxide, retrorsine, retrorsine N-oxide, senecionine, senecionine N-oxide, seneciphylline, seneciphylline N-oxide, senkirkine, senecivernine, senecivernine N-oxide, and trichodesmine were provided by Merck Chemicals (Milan, Italy). Standard stock solutions were prepared for each analyte (1 mg mL^{-1}) in MeOH and stored at -20 °C. Diluted solutions and standard mixtures were prepared in H_2O/MeOH 7:3 v/v.

2.2. PA-producing plants and samples

Ten PAs-producing plants, four of which belonging to the *Asteraceae* family (*Eupatorium cannabinum*, *Petasites hybridus*, *Senecio vulgaris*, *Tussilago farfara*) and the other six to the *Boraginaceae* family (*Anchusa officinalis*; *Borago officinalis*, *Echium italicum*, *Heliotropium europaeum*, *Lithospermum officinale*, *Symphytum officinale*) were provided by Giardino della Minerva (Orto botanico della Scuola Medica Salernitana, Salerno, Italy).

A total number of 282 commercial samples were analyzed. Honey (n = 72) and pollen (n = 6) samples from different botanical and geographical origins were obtained from Italian supermarkets, online shops, and local beekeepers. Herbal infusions (n = 101, including 21 labelled as dietary supplements),

black teas (n = 31), green teas (n = 20), and plant-based dietary supplements (n = 44 in solid form and n = 8 as syrups) were purchased from herbalist's and chemist's shops. Honey samples were stored at 4 °C until the analysis. Regarding herbal infusions, teas, and solid forms of plant-based dietary supplements, 50 % of units of each package were combined and milled to form a representative aggregate sample. Each aggregate sample was appropriately coded and kept in plastic containers at room temperature and protected from light until the analysis.

2.3. Sample preparation

The sample preparation procedure involved the aqueous extraction of PAs and PANOs followed by Salting-out Assisted Liquid-Liquid Extraction (SALLE). Honey samples were homogenized by manual stirring (3 min), and a representative aliquot of 25 g was diluted to 100 mL with distilled water and sonicated for 15 min (Rizzo, Celano, Campone, Rastrelli, & Piccinelli, 2022). Solid matrices (pollen and solid forms of dietary supplements) were extracted with an acidic water solution, according to Mulder and co-workers (Mulder et al., 2018). Briefly, 1 g of each sample was extracted with 20 mL (for pollen) and 10 mL (for dietary supplements) of acidic water (H_2SO_4, 0.05 M) by sonication (15 min) after vortex-mixing (1 min). The supernatant was collected after centrifugation (5 min at 13,000 rpm) and the solid residue was re-extracted under the same conditions. PA-producing plants were extracted with the same procedure used for solid matrices (1 g of plant with 20 mL of acidic water, twice). Herbal infusions, black and green teas were extracted according to the standardized procedure for teas and infusions (Mulder et al., 2018). In detail, 2 g of each homogenized sample were brewed with 150 mL of boiling water and left to infuse for 5 min. Then, the solution was filtered through a fluted filter paper. Syrups were properly diluted with water before being extracted.

Aqueous extracts of each matrix were subjected to the same SALLE procedure, according to our previous study (Rizzo et al., 2022). Briefly, a 10 mL aliquot of the aqueous solution was brought to a concentration of 1 M of $MgSO_4 \cdot 7H_2O$, 1.5 M Na_2SO_4, and to a pH value of 9.6; then, it was

centrifugated for 5 min (13,000 rpm). Afterwards, 2 mL of the aqueous solution were extracted with 2 mL of MeCN by vortexing the mixture for 1 min. The sample was then centrifugated for 5 min (13,000 rpm) to achieve the phase separation. The upper organic phase (MeCN) was quantitatively transferred into a clean tube and left to dry under a gentle nitrogen flow. Afterwards, the dried residue was redissolved with an appropriate volume of H_2O/MeOH 7:3 v/v: in 500 µL for honey, pollen, and solid forms of plant-based dietary supplements and 200 µL for herbal infusions and teas.

2.4 UHPLC-HRMS analysis

The analyses were conducted on an UltiMate 3000 UHPLC system (ThermoFisher Scientific, Milano, Italy) interfaced via a heated electrospray ionization source (HESI-II) to a Q-Exactive mass spectrometer (ThermoFisher Scientific, Milano, Italy). The UHPLC system was equipped with a Luna Omega Polar C18 (2.1 × 100 mm, 1.6 µm; Phenomenex, Bologna, Italy) column, operated at 40 °C with a flow rate of 400 µL min^{-1}. The chromatographic separation was achieved using a binary gradient of H_2O (A) and MeCN (B), both containing 0.1 % of formic acid; the elution gradient was as follows: 0–1 min, 2 % B; 1–5.5 min, 2–8 % B; 5.5–7.5 min, 8 % B; 7.5–9.5 min, 8–12 % B; 9.5–11 min, 12–18 % B; 11–13 min, 18–20 % B; 13–15 min, 20-40 % B; 15-17 min, 40-60 % B; 17-19 min, 60-80 % B. After each injection, washing (98 % B, 4 min) and re-equilibration of the column (2 % B, 5 min) were performed. The injection volume was set at 5 µL.

The mass spectrometer operated in positive ionization mode with the following instrument parameters: spray voltage, 3.5 kV; sheath gas flow rate, 50; auxiliary gas flow rate, 13; capillary and auxiliary gas heater temperatures, 300 °C; S-lens level, 55. Nitrogen was used as collision gas of the higher-energy collisional dissociation (HCD) cell. Data were acquired in Full MS/dd-MS^2 mode. The resolution of the Full MS scans (scan range 250-500 *m/z*) was set at 70k (FWHM), the Automatic Gain Control (AGC) target at 3e6, and the maximum IT (Injection time) at 250 ms. Each time the detector detected a peak corresponding to the accurate mass (± 5ppm) of a certain precursor ion of the inclusion list associated to the method, these ions were isolated in the quadrupole, accumulated

in the C-trap, and finally accelerated in the HCD cell to be fragmented. The inclusion list associated to the acquisition method was filled with 112 masses of precursor ions ($[M+H]^+$) (Table S1**)**. The fragmentation was performed using the NCE (Normalized Collision Energy) technology, which applies a stepped collisional energy scheme by combining low, medium, and high collision energies capable of increasing the diversity of fragment ions generated; a range of collision energies between 40 and 60 was applied in this study. The recording parameters of the dd-MS^2 scans were set as follows: mass resolution, 17.5 k (FWHM); AGC target, 2e4; maximum IT, 80 ms; isolation window, *m/z* 1.5; intensity threshold, 1.3e4; and dynamic exclusion: 2.0 s. The TopN parameter, which refers to the number of ions to be triggered after a Full MS scan, was disabled to prevent precursor ions other than those contained in the inclusion list from being isolated. Xcalibur software version 4.4 (ThermoFisher Scientific, Milano, Italy) was used for instrument control and data acquisition.

2.5. Data processing

The data processing was performed using TraceFinder software version 5.1 (ThermoFisher Scientific, Milano, Italy). In detail, two processing methods were built to automate and facilitate the data treatment, according to the specific objectives of the study. The first one, named as wide-scope suspect screening method, was developed to detect and characterize suspect PAs and PANOs from PAs-producing plants and commercial samples; the second one, named as high-throughput target screening and identification method, to rapidly perform the screening of a huge number of commercial samples regarding the presence of 118 target PAs and PANOs of the spectral library. Both the methods were created using the "Target screening method" workflow of the software.

2.5.1 Wide-scope suspect screening method

The Compound Database (CD) was built by importing a csv file, containing the list of 112 precursor ions of the inclusion list, associated with the instrumental acquisition method (Table S1), into the software. Then, 30 key product ions for the characterization of PAs and PANOs (*m/z* 120.0808,

138.0913, 150.0913, 168.1019, 124.1121, 142.1226, 122.0964, 140.107, 156.1019, 94.0651, 96.0808, 110.0964, 122.0964, 180.1019, 198.1125, 83.0491, 220.1332, 238.1438, 158.1176, 136.0757, 137.0835, 158.1176, 139.0992, 111.0679, 172.0968, 118.0651, 119.0729, 113.0835, 174.1125, 121.0886, 214.1074, 254.1387 (section 3.3.2) were associated with each precursor ion. A master method was then created with the following processing parameters: a range-integrated detection type over the entire chromatographic run; a response threshold (peak area) of 10e5; a mass tolerance of ± 5 ppm; and at least three product ions. The suspect compounds were flagged as "detected" (green flag) when all the criteria were fulfilled. This allowed the method to detect the presence of PAs/PANOs analogues whenever a peak matched the molecular formula of the relative precursor ion (± 5 ppm) and at least three diagnostic product ions (± 5 ppm) over the entire duration of the chromatographic run.

2.5.2 High-throughput target screening and identification method

The functioning of the high-throughput screening and identification method was linked to the construction of an in-house HRMS/MS spectral library. Therefore, the initial step involved the construction of the library, which was created using mzVault software version 2.3 (ThermoFisher Scientific, Milano, Italy) by uploading UHPLC-HRMS/MS information of the 118 target PAs and PANOs (Table 1). Then, the CD was built by importing into the master method a csv containing the acquired mass spectra information (retention time, molecular formula, precursor ions, five most abundant product ions and their ratios) of the 118 compounds of the library. The spectral library was associated to the processing method as additional identification tool. The following identification criteria were set: a retention time variation of ± 0.2 min, a response threshold of 10e4, a mass tolerance of 5 ppm for both precursor and product ions, a minimum of three product ions required for the identification, and a library match score higher than 70%. The target compounds were flagged as "identified" (green flag) when all the criteria were fulfilled, "found" when only the precursor ion was

encountered at the expected retention time (red flag), and "not found" (yellow flag) when none of the criteria were met.

2.6. Validation of the target screening and identification method

The high-throughput screening and identification method was validated in terms of specificity, accuracy (expressed as extraction efficiency, EE), limit of identification (LOI), and precision (expressed as false negative rates), according to the performance criteria of qualitative screening methods established by the European analytical guidelines (Magnusson & Örnemark, 2014; Pihlstrom et al., 2018). The validation studies were conducted on 28 out of 30 reference standards (indicine and indicine N-oxide were excluded for co-elution reasons) in six food matrices: honey, pollen, back and green teas, herbal infusions, and plant-based dietary supplements. The experiments were performed on blank samples, previously identified through analysis. A representative sample of herbal infusion was prepared by mixing the same amount of chamomile, fennel, melissa, mint, and licorice, as these herbs were the most encountered during the collection of the samples. On the contrary, it was not possible to select or prepare a representative sample of a plant-based dietary supplement due to the high variability of their composition. The specificity was evaluated by processing spiked (10 μg L^{-1}) and unspiked SALLE extracts of blank samples of each studied matrix. The EEs were determined by pre- and post-spiking the target analytes at a concentration of 10 μg L^{-1} of the SALLE extract (corresponding to 10 μg kg^{-1} for honey, 100 μg kg^{-1} for pollen, 75 μg kg^{-1} for teas and herbal infusions, and 50 μg kg^{-1} for dietary supplements) before and after the sample preparation procedure. Experiments were conducted in triplicate and EEs were calculated as area ratio of pre- and post-spiked samples. LOIs of herbal infusions, honey, pollen, black and green teas were evaluated by fortifying blank samples at eight concentration levels, ranging from 0.4 to 2 μg L^{-1} of the SALLE extracts. LOIs were assigned for each target analyte at the concentration level that met all the identification criteria of the high-throughput target screening and identification method (section 2.5.2). Regarding plant-based dietary supplements, since it was not possible to find a representative

sample, LOIs were estimated as the lowest concentration at which a compound was identified in at least 95 % of the blank samples. For this purpose, 20 blank samples (10 samples × 2 replicates) of different composition were spiked before the extraction at 10 and 20 µg kg^{-1}. The precision of the method, estimated as false negative rates, was determined by fortifying 72 blank samples (36 samples × 2 replicates), including honey samples (n = 3), pollen samples (n = 3), herbal infusions (n = 10), black (n = 5) and green (n = 5) teas, and dietary supplements (n = 10) at a concentration of 2 µg L^{-1} (corresponding to 2 µg kg^{-1} for honey, 20 µg kg^{-1} for pollen, 15 µg kg^{-1} for teas and herbal infusions, and 10 µg kg^{-1} for dietary supplements) and 4 µg L^{-1} (corresponding to 4 µg kg^{-1} for honey, 40 µg kg^{-1} for pollen, 30 µg kg^{-1} for teas and herbal infusions, and 20 µg kg^{-1} for dietary supplements) of the SALLE extracts, which correspond to the tenth and the fifth part of the lower limit of the Regulation (EU) 2020/2040 (Tea, *Camellia sinensis*, ML of 150 µg kg^{-1}).

3. Results and discussion

3.1 UHPLC-HRMS/MS analysis

The setting of the UHPLC conditions aimed at solving/minimizing one of the main problems encountered during the chromatographic analysis of PAs and PANOs, that is the co-elution of structural isomers impossible to distinguish by their MS/MS spectra. Some examples of these similarities are offered by the isomeric groups indicine/intermedine/lycopsamine, echinatine/rinderine, integerrimine/senecionine/senecivernine, echimidine/heliosupine, seneciphylline/spartioidine, and their N-oxides (Casado et al., 2022; Kaltner, Stiglbauer, Rychlik, Gareis, & Gottschalk, 2019). Therefore, the chromatographic conditions were carefully optimized on both the 30 reference standards and the extracts of the 10 PA-producing plants to obtain a better resolution of the peaks. Thus, it was possible to obtain the separation of both structural isomers of the reference standards and further isomers. As already reported by Kaltner and co-workers, the best chromatographic separation conditions of the isomers are obtained using acidified solvents (Kaltner et al., 2019). The optimized conditions allowed to achieve a good separation for most of the abovementioned PAs and PANOs isomers, within a run time of 17 min. In addition, many of the indistinguishable structural isomer pairs, characterized from the extracts of PA-producing plants, (7-acetylintermedine/7-acetyllycopsamine, amabiline/supinine, asperumine/heliosupine, lasiocarpine/7-tigloyleuropine, their N-oxides, and neosenkirkine/senkirkine) resulted in well separated peaks. Indicine/lycopsamine and their N-oxides and integerrimine/senecionine or senecivernine were the only isomers that couldn't be resolved. Even the isomers putatively identified as echinatine and rinderine, their 7-acetyl analogues, and their N-oxides were not sufficiently resolved under the chromatographic conditions used.

Different HRMS/MS acquisition modes were considered to evaluate the suitability of the detection method to the structural characterization and identification of PAs. Eventually, a data-dependent acquisition mode (Full MS/dd-MS^2), with an inclusion list of prioritised masses, was selected as it proved to be efficient in terms of selectivity and ability to detect the target analytes at trace levels and

provide high quality HRMS/MS spectra. The quality of the MS/MS spectra is crucial to obtain reliable identifications of molecules in complex matrices, and the data-dependent acquisition mode provides MS/MS spectra from specific precursor ions by dismissing the other precursor ions, which reduces the risk of background noise and signal interferences (Rajski et al., 2021).

The Full MS/dd-MS^2 was adapted to the detection and characterization of a wide range of PAs at low concentration levels (ppb) in complex food matrices. For this purpose, the mass range of the Full MS scan (*m/z* 250-550) was defined to cover the entire range of molecules of the internal database (section 3.3.1). The dd-MS^2 scan was triggered on an inclusion list of accurate masses of $[M+H]^+$ ions obtained from the internal database. This allowed to fragment the suspected PAs over matrix-interfering ions, even when they were present as minor compounds. The TopN function, which selects the most abundant ions of every single Full MS scan, was disabled as it is not suitable for trace analyses in complex matrices; in fact, in such conditions, the selected ions would correspond to the matrix interferences. Furthermore, to detect and confirm the target analytes at low contamination levels, the minimum AGC target of the dd-MS^2 scan was set to a much lower value (10e3) than that commonly used in Full MS/dd-MS^2 analyses (10e5-10e6). The optimal collision energies were determined by analyzing the reference standards to obtain fragmentation spectra with significant product ions. The developed acquisition method allowed to detect (Full MS) and identify (dd-MS^2) target PAs and PANOs up to a concentration close to 1 μg L^{-1}, with enough data points across the chromatographic peaks (Full MS extracted ion chromatogram) and reliable fragmentation profiles.

3.2 Sample preparation

The development of a sample preparation procedure is challenging for trace-level analysis in complex matrices. Considering the objectives of the study, a simple, quick, and cheap sample preparation procedure was carried out. The simultaneous aqueous extraction of PAs and PANOs from the investigated matrices was performed before subjecting the samples to SALLE, which was used as clean-up step. All the solid matrices (honey, pollen, and solid forms of plant-based dietary

supplements) were extracted with acidified water, an extensively used solvent for the extraction of these alkaloids from different food matrices due to the ability to provide exhaustive extraction and cleaner extracts (Casado et al., 2022; Kaltner et al., 2019; Mulder et al., 2018). Teas and herbal infusions were extracted by infusion with boiling water to simulate the real exposure scenario to these contaminants (Casado et al., 2022; Mulder et al., 2018; Picron et al., 2018). The SALLE procedure previously developed for the determination of nine PAs and PANOs in honey and pollen (Rizzo et al., 2022) was adapted to be applied to further food matrices and a larger pool of analytes (15 PAs and 13 PANOs). The optimization of the sample preparation procedure was performed by fortifying the tested matrices at 10 $\mu g\ L^{-1}$ of each analyte in SALLE extracts (this level corresponds to 10 $\mu g\ kg^{-1}$ for honey, 100 $\mu g\ kg^{-1}$ for pollen, 75 $\mu g\ L^{-1}$ for teas and herbal infusions, 50 $\mu g\ L^{-1}$ for dietary supplements). The performances of the procedure were evaluated in terms of extraction efficiency. Under optimal conditions, the procedure provided exhaustive EEs (69-113 %) (Table 2). The SALLE procedure was also applied to aqueous extracts of PA-producing plants to evaluate its efficiency in extracting PAs and PANOs others than the target ones. No differences were observed between the profiles of the aqueous and SALLE extracts, indicating the efficiency of the procedure in extracting naturally occurring PAs and PANOs from PA-producing plants.

3.3 Identification strategy

PAs show a striking variety of chemical structures being the result of the combination of a limited set of necine bases and many necic acids. The structural diversity of PAs is further amplified by the type of ester linkage, acetylation, and hydroxylation of necic acids, and the oxidation of the amino group. Moreover, necine bases can either be fully saturated or 1,2-unsaturated. Based on the necine bases commonly found in plants, PAs can be classified into six groups: retronecine (R), heliotridine (H), otonecine (O), supinidine (S), platynecine (P) and trachelanthamidine (T) types (Fig. S1). The first four types are 1,2-unsaturated PAs, while the types P and T are the corresponding saturated derivatives of the R/H and S types, respectively. Except for the O type, in which N-oxides cannot be

356 formed, N-oxides of the other types of necine bases naturally occur and often coexist with their PA
357 form in plant materials. Depending on the linkage between the necine base and the necic acids, PAs
358 can also be divided into monoesters (m), cyclic diesters (c) and open-chained diesters (d). In PA
359 diesters, limited to R, H, O, and P types, the esterification occurs at C-7 and C-9 and cyclic diesters
360 derive from the esterification of the necine base with dicarboxylic necic acids (EFSA, 2011; Moreira
361 et al., 2018; Schramm et al., 2019).
362
363 *3.3.1 Database of PAs and PANOs*
364 A wide database of PAs and PANOs was created from a systematic survey of the literature to support
365 the identification strategy. The list of known compounds was also implemented with "expected
366 unknowns", intended as unreported compounds that can be predicted based on the chemical features
367 of this class of alkaloids (e. g. N-oxide derivatives). The database (778 molecules) was filled with
368 structural information (CAS number, elemental composition, molecular weight, accurate mass of
369 precursor ions), and the groups of PAs with identical molecular formula were further classified into
370 different subgroups according to the N-oxidation, the necine base and the type of esterification (Table
371 S2).
372
373 *3.3.2 Diagnostic product ions filtering strategy*
374 The structural diversity of PAs appears in the fragmentation patterns that emerge from tandem mass
375 spectrometry. Depending on the type of necine base, necic acids, esterification type and N-oxidation
376 of the pyrrolizidine ring, PAs and PANOs show characteristic and predictable product ions with
377 specific ion ratios. This behavior was used to develop a HRMS/MS approach for their detection and
378 characterization without the need for reference standards. Thus, a diagnostic product ion filtering
379 strategy was designed for the characterization of PAs and PANOs through their HRMS/MS spectra.
380 A systematic flowchart (Fig. 1) was designed to delineate the fragmentation patterns of PAs and
381 PANOs by studying the HRMS/MS spectra of the reference standards, online spectral libraries, and

previous studies (Mädge, Gehling, Schöne, Winterhalter, & These, 2020; Ruan et al., 2012; These, Bodi, Ronczka, Lahrssen-Wiederholt, & Preiss-Weigert, 2013). Important clarifications regarding the ion ratios arose during the collection of HRMS/MS spectra of the spectral library. The Fig. S2 and S3 show the chemical structures, molecular formulas, and exact masses of the key product ions required for the subdivision of PAs and PANOs into the different groups and subgroups of the Fig. 1. The flowchart was divided in two subsets since the HRMS/MS spectra immediately allowed to differentiate PAs (Fig. 1A) from PANOs (Fig. 1B).

The different necine base types of PAs are easily recognized by the presence of characteristic product ions: *m/z* 120.0808 and 138.0910 for both R and H types, *m/z* 150.0913 and 168.1019 for O type, *m/z* 122.0964 and 140.1070 for both P and S types, and *m/z* 124.1121 and 142.1226 for T type (Fig. 1A). The product ions of higher intensity were placed on the top of each subset by adding in succession characteristic product ions for each subgroup as far as it was possible. Regarding R and H types, PA monoesters are easily distinguished from diesters as they show the distinctive product ion at *m/z* 156.1019. Depending on the base peak, monoesters can be differentiated into R (bp at *m/z* 94.0654) and H types (bp at *m/z* 138.0910). Cyclic and open-chained diesters of R/H type can be differentiated based on the relative intensity of the product ions at *m/z* 94.0654, 120.0808, and 138.0910: they show comparable intensities (> 20%) in cyclic forms, and a base peak at *m/z* 120.0808 and low intensities (< 10%) at *m/z* 94.0651 and 138.0913 in open-chained diester forms. The presence of product ions at *m/z* 180.1019 and 198.1125 identify an acetyl group at C-7 while product ions at *m/z* 83.0491, 220.1332, and 238.1438 identify an angeloyl/tigloyl group at the same position. Regarding S types, the product ions at *m/z* 94.0654 and 110.0964 are crucial for their identification (Fig. 1A).

PANOs show more complex HRMS/MS spectra than PAs and characteristic product ion clusters (Fig. 1B). The cluster 136 *to* 138 (*m/z* 136.0757, 137.0835, and 138.0913) identifies R and H PANOs. Whitin R and H types, the base peak at *m/z* 172.0968 and the product ion at *m/z* 111.0679 identify the monoester subgroups and allow to distinguish them from the diester subgroups, which show the cluster 118 *to* 120 (*m/z* 118.0651, 119.0729, and 120.0808). Depending on the relative intensities of

the cluster 136 *to* 138, monoesters can be differentiated into R (higher intensities) and H (lower intensities) types. The same applies to open-chained diesters, albeit in inverted ratios. In both groups, the product ions at *m/z* 214.1074 or 254.1387 indicate the presence of an acetyl or angeloyl/tigloyl group respectively at the C-7 position of the open-chained diesters. S and P types of PANOs are instead characterized by the cluster 138 *to* 140 (*m/z* 138.0913, 139.0992, and 140.1070); the base peak at *m/z* 156.1019 and the product ion at *m/z* 139.0992 allow to differentiate S from P types (Fig. 1B).

3.3.2.1 Wide-scope suspect screening method

After delineating the spectral features of PAs and PANOs, A reliable informatic solution was elaborated to handle with the large amount of HRMS/MS data and to automate and facilitate the detection and characterization of PAs and PANOs. The wide-scope suspect screening method was developed by associating each precursor ion of the inclusion list to a set of diagnostic product ions (section 2.5.1). This allowed the software to process the raw data, flagging as putative PAs/PANOs the only peaks with a molecular formula corresponding to that of the compounds of the database (± 5 ppm) and at least three diagnostic product ions (± 5 ppm) (Fig. 2). The product ions (*m/z* values and ion ratios) of suspected peaks were first matched with the information reported in the flowchart (Fig. 1) to establish the group and subgroup of the detected compound, and then the presumed structures were searched into the database (Table S2) to verify the match with a collected analogue. The presumed identity of the detected PA/PANO was confirmed by comparison with the reference standards (MSI, L1 – Metabolomics Standards Initiative, Level 1), or putatively assigned based on literature studies and online databases (MSI, L2). When no spectrum or literature information was available, the detected PA/PANO was tentatively assigned to the compound suggested by the proposed identification strategy, when present (MSI, L3). Fig. 2 shows three examples of application of the diagnostic product ions filtering strategy during the identification of suspect PAs.

3.4 HRMS/MS spectral library

The diagnostic product ions filtering strategy was applied to 10 PAs-producing plants to detect and identify as much compounds as possible and collect their spectra into an HRMS/MS spectral library. The plant profiles (Table S3) were defined by comparing the information of the diagnostic product ions filtering strategy with literature information, MS/MS spectra available on online databases and libraries, and chemotaxonomic data. The latter resulted essential in discriminating structural isomers with superimposable MS/MS spectra (echiumine in *Echium italicum*, echinatine/rinderine in *Eupatorium cannabinum*, heliosupine in *Heliotropium europaeum*, and symphytine in *Symphytum officinale*). 84 PAs and PANOs other than the reference standards were detected, including two "expected unknowns": canescine/canescenine N-oxide (*m/z* 416.2275, $C_{20}H_{34}NO_8^+$) and lithosenine N-oxide (*m/z* 432.2223, $C_{20}H_{34}NO_9^+$) in *L. officinale*. Their structures, hypothesized on the basis of the key product ions of R/H open-chained diester type of PANOs (Fig. S4), were further supported by chemotaxonomic data (El-Shazly & Wink, 2014; Kopp, Abdel-Tawab, & Mizaikoff, 2020). Moreover, the product ion at *m/z* 272.1492 ($C_{13}H_{22}NO_5^+$) corresponds to a hydroxyisovaleroyl residue (typical necic acid of canescine and lithosenine) at the C-7 position. Besides, the clusters at *m/z* 136 *to* 138 in the spectra of lithosenine N-oxide (low intensity; < 50%) and canescine N-oxide (high intensity; > 50%) further supported their assignments as R and H types, respectively (Fig. 1B).

A spectral library of 114 total compounds was built (Table 1). Among these, 30 were reference standards (MSI, L1), 52 were putatively assigned based on their MS similarity with literature information and online databases (MSI, L2), and 32 were assigned based on the diagnostic product ions filtering strategy and chemotaxonomic data (MSI, L3). During the analysis of the commercial samples, four further compounds were characterized, bringing the number of spectra of the library to 118. The library includes all the PAs of the EFSA's list (28) and the Regulation 2020/2040/EU (21). 103 out of 118 compounds are 1,2 unsaturated PAs, of which the 58 % are R type and the 34 % are H type.

3.5 High-throughput target screening and identification method

The in-house spectral library was then associated to the high-throughput target screening and identification method. The identification criteria were set as follows: the presence of the precursor, a mass tolerance < ± 5 ppm, the expected retention time (± 0.2 min), at least three product ions (± 5 ppm), and a library match score higher than 70%. This post-acquisition data evaluation was combined with the optimized sample preparation procedure and PA-tailored UHPLC-HRMS/MS method for the analysis of numerous PAs in food matrices with high risk of contamination. Fig. 3 shows an example of the method ability to identify europine N-oxide and distinguish it from a close interfering peak in a dietary supplement sample. As can be seen, europine N-oxide (Fig. 3A) met all the identification criteria (mass tolerance of the precursor ion, 0.7 ppm; 4 product ions with mass tolerance < 5 ppm; library match score, 86 %), while the interfering peak (Fig. 3B) only met two of them (mass tolerance of precursor ion, 0.5 ppm; retention time within the range). These results highlight that the most stringent identification criteria were those related to the HRMS/MS data and demonstrate the efficacy of the identification method in detecting the target PAs and PANOs of the library with high reliability.

3.6 Qualitative analytical performance

A qualitative validation was performed since the aim of the proposed study was to develop an analytical platform for the detection and identification of PAs in complex matrices at relevant contamination levels. The method specificity, LOIs, and precision (false negative rate) were evaluated on 28 reference standards for all the investigated matrices, according to the performance criteria of screening methods (Magnusson & Örnemark, 2014; Pihlstrom et al., 2018). Regarding the remaining PAs and PANOs, for which no reference standards were available, the detection and identification can be achieved although it is not possible to specify qualitative performance parameters (Pihlstrom et al., 2018).

485 The method specificity, defined as the ability of the method to distinguish the analyte from any other
486 matrix interferences, was evaluated by comparison between different blank and spiked samples of the
487 studied matrices. No interfering peaks were observed at the expected retention time for all the 28
488 reference standards in honey and pollen samples. On the contrary, some plant-based samples showed
489 the presence of interfering peaks close to the some of the target analytes. The proposed method
490 provided satisfactory specificity and the matrix interferents were either chromatographically or
491 spectrally discriminated; moreover, the number of false positives dropped to zero when all the
492 identification criteria were considered.
493 To achieve an accurate identification of the target analytes and minimize the risk of false positives,
494 diagnostic information, that meets the defined criteria, is required (Lehotay, Sapozhnikova, & Mol,
495 2015). The LOIs, defined as the lowest concentration that fulfill all the identification criteria of the
496 method, were established to estimate the threshold concentrations at which the identification become
497 reliable. LOIs of the 28 target analytes in the six tested matrices ranged from 0.6 to 30 μg kg^{-1} (Table
498 2). The method was able to detect and identify all the target analytes in the SALLE extract at a
499 concentration of 2 μg L^{-1}, except for echimidine, echimidine N-oxide, erucifoline, jacobine,
500 monocrotaline, retrorsine, retrorsine N-oxide, seneciphylline N-oxide, senecivernine, senecivernine
501 N-oxide, which were detected from 4 μg L^{-1} in dietary supplements. The LOIs demonstrated to be
502 fit-for-purpose regarding PA-monitoring applications; LOIs were much lower than the MLs (17-119
503 times in pollen, 21-67 times in herbal infusion, 10-50 times in tea, and 20-40 times in dietary
504 supplement).
505 The precision of the method was calculated as false negative rate. Considering the calculated LOIs
506 and the regulatory MLs, two cut-off levels, 2 and 4 μg L^{-1} of the SALLE extract, were defined to
507 achieve the best suited false negative rate; the guidelines require identification methods to accomplish
508 a false negative rate ≤ 5% (Lehotay et al., 2015). The overall false negative rate evaluated on 36 blank
509 samples spiked at the two abovementioned levels and processed in duplicates, was lower than 5 %
510 (0-1.3 %) at 4 μg L^{-1} of the SALLE extract for all the 28 analytes. However, the method achieved

511 reliable identification results (< 5 % of false negatives) at the lowest level tested (2 µg L^{-1}) as well
512 for most of the analytes, excluding those with a LOI of 20 µg kg^{-1} in dietary supplements (Table 2)
513 and erucifoline N-oxide, senecionine, seneciphylline and senecivernine in teas and infusions.
514
515 **3.7 Analysis of commercial samples**
516 A huge number of commercial samples (n = 282) was screened against the 118 target PAs and PANOs
517 to demonstrate the applicability of the analytical platform and investigate the profile of different food
518 matrices. The collected samples represent food matrices susceptible to the contamination of PAs and
519 relevant to consumer intake; they include honey, pollen, black and green teas, herbal infusions, and
520 plant-based dietary supplements. Qualitative data only are discussed in this study as further studies
521 will be necessary to test the suitability of the procedure for the quantitative determination of the
522 analytes in the studied matrices and validate it accordingly.
523 The wide-scope suspect screening method was applied to the commercial samples to interrogate them
524 regarding the presence of PAs and PANOs other than those already characterized from PA-producing
525 plants. This allowed to detect four additional PAs: helioamplexine and two isomers of echimidine in
526 honey samples, and acetylseneciphylline N-oxide in a dietary supplement, which were added to the
527 HRMS/MS spectral library and to the high-throughput screening and identification method.
528 The qualitative analysis of the samples revealed the presence of 60 PAs/PANOs in 59 % of the
529 analyzed samples (Table S4); among these, 21 PAs/PANOs were listed in the 2040/2020/EU
530 Regulation (echimidine, europine, heliotrine, intermedine, lasiocarpine, lycopsamine, retrorsine,
531 senecionine, seneciphylline, senecivernine, their N-oxides, and senkirkine), 8 belonged to the list of
532 14 coeluting isomers to be monitored (echinatine, heliosupine, indicine, integerrimine, rinderine,
533 spartioidine, usaramine, and their N-oxides) and 28 were PAs included in the HRMS/MS spectral
534 library but not mentioned in the Regulation or in the EFSA's list of relevant contaminants of plant
535 matrices. Among the studied matrices, honey was found to be the most contaminated one as 89 % of
536 the samples tested positive to the presence of PAs. In decreasing order of contamination, follow

dietary supplements (58 %), pollen (50 %), herbal infusions (46 %), and teas (39 %). Regarding the contamination profile, Fig. 4 shows the PAs and PANOs detected in honey, herbal infusions, and plant-based dietary supplements, which turned out to be the matrices with the widest profiles of contamination (32, 34 and 49 analytes detected, respectively). In detail, the most frequently detected and identified compounds (> 20 % of the contaminated samples of each matrix) were echimidine and its two isomers, echimidine N-oxide, echinatine/rinderine, 5-hydroxyindicine, intermedine, lycopsamine, and symphytines for honey; europine N-oxide, heliotrine N-oxide, lasiocarpine N-oxide, and senecionine N-oxide for herbal infusions; and echinatine/rinderine, europine, heliotrine, heliotrine N-oxide, lasiocarpine, and senecionine for dietary supplements. The qualitative data on the distribution of PAs indicated that the PAs and PANOs of the Regulation 2040/2020/EU contribute to almost the total content for herbal infusions (86 %) and dietary supplements (83 %). On the other hand, 47 % of the PAs detected in honey were not included in the lists of relevant PAs to be monitored; echimidine isomer 1 (55 %) and 2 (59 %), 5-hydroxyindicine (41 %) and the sum of symphytines 1 and 2 (22 %) were the most prevalent.

3.8 Conclusions

The present study proposes an analytical platform for the rapid and automated detection of pyrrolizidine alkaloids in food matrices with high risk of contamination. It consists of an easy and cheap sample preparation followed by a PA-tailored UHPLC-HRMS/MS analysis, which combined with the identification strategy and a post-acquisition data evaluation allow to detect, identify, and characterize a wide range of compounds at the required levels.

This analytical platform offers the possibility to interrogate the samples on the presence of the 118 target PAs and PANOs of the target screening method, and to identify additional unreported analogues. The complementary mode of operation of the wide-scope suspect screening method and the high-throughput target screening and identification method makes the procedure versatile and

562 state-of-the-art. The HRMS/MS spectral library can be continuously implemented with newly
563 identified compounds according to the proposed strategy.
564 Furthermore, the possibility of adding further molecular masses to the inclusion list of the Full
565 MS/dd-MS^2 acquisition method, each time a PA is identified, allows to considerably broaden the
566 identification range since each molecular mass can identify multiple structural isomers. Finally, the
567 non-dependence of the platform on the purchase of reference standards not only lowers the cost of
568 the procedure but also solves the problem of the lack of reference standards of these toxins.
569 Further studies are underway to evaluate the suitability of the proposed analytical procedure for the
570 determination of the PA levels in high-risk food matrices and validate it accordingly.
571

CRediT author statement

Serena Rizzo: Conceptualization; Data curation; Formal analysis; Investigation; Methodology; Software; Validation; Visualization; Roles/Writing - original draft; Writing - review & editing. **Rita Celano**: Conceptualization; Investigation; Methodology; Supervision; Validation; Roles/Writing - original draft; Writing - review & editing. **Simona Serio**: Formal analysis; Software. **Anna Lisa Piccinelli**: Conceptualization; Data curation; Methodology; Project administration; Resources; Software; Supervision; Validation; Visualization; Roles/Writing - original draft; Writing - review & editing. **Mariateresa Russo**: Conceptualization; Funding acquisition; Writing - review & editing. **Luca Rastrelli**: Conceptualization; Funding acquisition; Project administration; Resources; Writing - review & editing.

582 **References**

583 Casado, N., Morante-Zarcero, S., & Sierra, I. (2022). The concerning food safety issue of
584 pyrrolizidine alkaloids: An overview. *Trends in Food Science and Technology*, *120*, 123–139.
585 https://doi.org/10.1016/j.tifs.2022.01.007

586 Dusemund, B., Nowak, N., Sommerfeld, C., Lindtner, O., Schäfer, B., & Lampen, A. (2018). Risk
587 assessment of pyrrolizidine alkaloids in food of plant and animal origin. *Food and Chemical*
588 *Toxicology*, *115*(March), 63–72. https://doi.org/10.1016/j.fct.2018.03.005

589 EFSA. (2011). Scientific Opinion on Pyrrolizidine alkaloids in food and feed. *EFSA Journal*, *9*(11),
590 2406; 1–134. https://doi.org/10.2903/j.efsa.2011.2406

591 EFSA. (2016). Dietary exposure assessment to pyrrolizidine alkaloids in the European population.
592 *EFSA Journal*, *14*(8), 4572; 50 pp. https://doi.org/10.2903/j.efsa.2016.4572

593 EFSA. (2017). Risks for human health related to the presence of pyrrolizidine alkaloids in honey,
594 tea, herbal infusions and food supplements. *EFSA Journal*, *15*(7), 4908, 34 pp.
595 https://doi.org/10.2903/j.efsa.2017.4908

596 El-Shazly, A., & Wink, M. (2014). Diversity of pyrrolizidine alkaloids in the Boraginaceae
597 structures, distribution, and biological properties. *Diversity*, *6*(2), 188–282.
598 https://doi.org/10.3390/d6020188

599 European Commission. (2020). Commission Regulation (EU) 2020/2040 of 11 December 2020
600 amending Regulation (EC) No 1881/2006 as regards maximum levels of pyrrolizidine
601 alkaloids in certain foodstuffs (Text with EEA relevance). *Official Journal of the European*
602 *Union*, L 420/1-5.

603 Hird, S. J., Lau, B. P. Y., Schuhmacher, R., & Krska, R. (2014). Liquid chromatography-mass
604 spectrometry for the determination of chemical contaminants in food. *TrAC - Trends in*
605 *Analytical Chemistry*, *59*, 59–72. https://doi.org/10.1016/j.trac.2014.04.005

606 Kaltner, F., Stiglbauer, B., Rychlik, M., Gareis, M., & Gottschalk, C. (2019). Development of a
607 sensitive analytical method for determining 44 pyrrolizidine alkaloids in teas and herbal teas

via LC-ESI-MS/MS. *Analytical and Bioanalytical Chemistry*, *411*(27), 7233–7249. https://doi.org/10.1007/s00216-019-02117-1

Kopp, T., Abdel-Tawab, M., & Mizaikoff, B. (2020). Extracting and analyzing pyrrolizidine alkaloids in medicinal plants: A review. *Toxins*, *12*(5), 7–10. https://doi.org/10.3390/toxins12050320

Lehotay, S. J., Sapozhnikova, Y., & Mol, H. G. J. (2015). Current issues involving screening and identification of chemical contaminants in foods by mass spectrometry. *TrAC - Trends in Analytical Chemistry*, *69*, 62–75. https://doi.org/10.1016/j.trac.2015.02.012

Ma, C., Liu, Y., Zhu, L., Ji, H., Song, X., Guo, H., & Yi, T. (2018). Determination and regulation of hepatotoxic pyrrolizidine alkaloids in food: A critical review of recent research. *Food and Chemical Toxicology*, *119*, 50–60. https://doi.org/10.1016/j.fct.2018.05.037

Mädge, I., Gehling, M., Schöne, C., Winterhalter, P., & These, A. (2020). Pyrrolizidine alkaloid profiling of four Boraginaceae species from Northern Germany and implications for the analytical scope proposed for monitoring of maximum levels. *Food Additives and Contaminants - Part A Chemistry, Analysis, Control, Exposure and Risk Assessment*, *37*(8), 1339–1358. https://doi.org/10.1080/19440049.2020.1757166

Magnusson, B., & Örnemark, U. (2014). *Eurachem Guide: The Fitness for Purpose of Analytical Methods – A Laboratory Guide to Method Validation and Related Topics*. *Eurachem*. https://doi.org/10.1016/S0014-2999(99)00500-2

Menger, F., Gago-Ferrero, P., Wiberg, K., & Ahrens, L. (2020). Wide-scope screening of polar contaminants of concern in water: A critical review of liquid chromatography-high resolution mass spectrometry-based strategies. *Trends in Environmental Analytical Chemistry*, *28*, e00102. https://doi.org/10.1016/j.teac.2020.e00102

Moreira, R., Pereira, D. M., Valentão, P., & Andrade, P. B. (2018). Pyrrolizidine alkaloids: Chemistry, pharmacology, toxicology and food safety. *International Journal of Molecular Sciences*, *19*(6). https://doi.org/10.3390/ijms19061668

Mulder, P. P. J., López, P., Castelari, M., Bodi, D., Ronczka, S., Preiss-Weigert, A., & These, A. (2018). Occurrence of pyrrolizidine alkaloids in animal- and plant-derived food: results of a survey across Europe. *Food Additives and Contaminants - Part A Chemistry, Analysis, Control, Exposure and Risk Assessment*, *35*(1), 118–133. https://doi.org/10.1080/19440049.2017.1382726

Picron, J. F., Herman, M., Van Hoeck, E., & Goscinny, S. (2018). Analytical strategies for the determination of pyrrolizidine alkaloids in plant based food and examination of the transfer rate during the infusion process. *Food Chemistry*, *266*(June), 514–523. https://doi.org/10.1016/j.foodchem.2018.06.055

Pihlstrom, T., Fernández-Alba, A. R., Gamón, M., Amate, C. F., Poulsen, M. E., Lippold, R., & Anastassiades, M. (2018). Analytical quality control and method validation procedures for pestice residues analysis in food and feed. *Sante/11813/2017*, 42.

Rajski, Ł., Petromelidou, S., Díaz-Galiano, F. J., Ferrer, C., & Fernández-Alba, A. R. (2021). Improving the simultaneous target and non-target analysis LC-amenable pesticide residues using high speed Orbitrap mass spectrometry with combined multiple acquisition modes. *Talanta*, *228*(January). https://doi.org/10.1016/j.talanta.2021.122241

Righetti, L., Paglia, G., Galaverna, G., & Dall'Asta, C. (2016). Recent advances and future challenges in modified mycotoxin analysis: Why HRMS has become a key instrument in food contaminant research. *Toxins*, *8*(12). https://doi.org/10.3390/toxins8120361

Rizzo, S., Celano, R., Campone, L., Rastrelli, L., & Piccinelli, A. L. (2022). Salting-out Assisted Liquid-Liquid Extraction for the rapid and simple simultaneous analysis of pyrrolizidine alkaloids and related N-oxides in honey and pollen. *Journal of Food Composition and Analysis*, *108*(October 2021), 104457. https://doi.org/10.1016/j.jfca.2022.104457

Ruan, J., Li, N., Xia, Q., Fu, P. P., Peng, S., Ye, Y., & Lin, G. (2012). Characteristic ion clusters as determinants for the identification of pyrrolizidine alkaloid N-oxides in pyrrolizidine alkaloid-containing natural products using HPLC-MS analysis. *Journal of Mass Spectrometry*, *47*(3),

331–337. https://doi.org/10.1002/jms.2969

Schramm, S., Köhler, N., & Rozhon, W. (2019). Pyrrolizidine alkaloids: Biosynthesis, biological activities and occurrence in crop plants. *Molecules*, *24*(3), 1–44. https://doi.org/10.3390/molecules24030498

Schrenk, D., Gao, L., Lin, G., Mahony, C., Mulder, P. P. J., Peijnenburg, A., … These, A. (2020). Pyrrolizidine alkaloids in food and phytomedicine: Occurrence, exposure, toxicity, mechanisms, and risk assessment - A review. *Food and Chemical Toxicology*, *136*(November 2019), 111107. https://doi.org/10.1016/j.fct.2019.111107

Steinhoff, B. (2019). Pyrrolizidine alkaloid contamination in herbal medicinal products: Limits and occurrence. *Food and Chemical Toxicology*, *130*(September 2018), 262–266. https://doi.org/10.1016/j.fct.2019.05.026

These, A., Bodi, D., Ronczka, S., Lahrssen-Wiederholt, M., & Preiss-Weigert, A. (2013). Structural screening by multiple reaction monitoring as a new approach for tandem mass spectrometry: Presented for the determination of pyrrolizidine alkaloids in plants. *Analytical and Bioanalytical Chemistry*, *405*(29), 9375–9383. https://doi.org/10.1007/s00216-013-7365-4

Figures captions.

Fig. 1. Flowchart of key product ions for the identification of pyrrolizidine alkaloids (A) and their N-oxides (B).

Fig. 2. Mode of operation of the diagnostic product ions filtering strategy for the identification of (A) senkirkine (MSI, L1), (B) heliosupine N-oxide (MSI, L2), and (C) thesinine (MSI, L3).

Fig. 3. Specificity of the high-throughput target screening and identification method in (A) identifying europine N-oxide and (B) distinguishing it from a close interfering peak in a dietary supplement.

Fig. 4. Contamination profiles of (A) honey, (B) herbal infusions, and (C) dietary supplements. The percentage on each bar represents the prevalence of each PA/PANO in positive samples. Only PAs present in more than 5 % of the positive samples are shown.

689 **Table 1.** HRMS/MS spectral library of the 118 target PAs and PANOs.

Name [a]	Necine base [b]	Necic acid [c]	Molecular formula	$[M+H]^+$ (m/z) [d]	TR (min)	Diagnostic product ions, m/z (relative abudance)	IL [e]
7-Tigloylretronecine NO	R	m	$C_{13}H_{19}NO_4$	254.1387	7.2	106.0653 (100); 83.0496 (34); 111.0679 (28); 136.0757 (21); 94.0654 (18)	2
7-Angeloylretronecine NO	R	m	$C_{13}H_{19}NO_4$	254.1387	7.4	106.0654 (100); 83.0496 (46); 136.0758 (32); 94.0655 (31); 111.0680 (30)	2
9-Tigloylretronecine NO	R	m	$C_{13}H_{19}NO_4$	254.1387	10.4	93.0577 (88); 136.0757 (77); 138.0913 (35); 137.0833 (30); 94.0654 (30); 108.0809 (20)	2
9-Angeloylretronecine NO	R	m	$C_{13}H_{19}NO_4$	254.1387	10.7	93.0577 (93); 136.0757 (66); 154.0861 (56); 83.0496 (46); 94.0654 (36); 137.0834 (34); 138.0913 (33)	2
Supinine	S	-	$C_{15}H_{25}NO_4$	284.1856	8.1	122.0965 (100); 140.1069 (66); 70.0657 (23); 110.0967 (12); 94.0655 (11)	2
Amabiline	S	-	$C_{15}H_{25}NO_4$	284.1856	8.4	122.0964 (100); 140.1069 (90); 70.0657 (28); 110.0967 (16); 94.0655 (13)	2
Spilanthine	T	-	$C_{15}H_{25}NO_4$	284.1856	9.2	142.1227 (100); 124.1122 (56); 96.0811 (8); 70.0657 (6)	2
Viridiflorine	T	-	$C_{15}H_{27}NO_4$	286.2013	7.9	142.1227 (100); 125.1198 (7); 70.0657 (6); 124.1121 (5); 96.0814 (1)	2
Cynaustraline	T	-	$C_{15}H_{27}NO_4$	286.2013	8.2	142.1225 (100); 124.1120 (52); 70.0657 (12); 86.0968 (9); 96.0810 (5)	2
Thesinine	T	-	$C_{17}H_{21}NO_3$	288.1594	13.7	147.0441 (100); 142.1227 (40); 124.1122 (39); 119.0493 (18); 96.0812 (5)	3
Heleurine	S	-	$C_{16}H_{27}NO_4$	298.2013	12.0	122.0965 (100); 140.1069 (57); 94.0655 (13); 110.0966 (12); 70.0657 (11)	2
Intermedine	R	m	$C_{15}H_{25}NO_5$	300.1805	5.3	94.0654 (100); 156.1018 (47); 138.0912 (39); 120.0807 (16); 82.0656 (7)	1
Indicine	R	m	$C_{15}H_{25}NO_5$	300.1805	5.5	94.0654 (100); 156.1016 (46); 138.0912 (35); 120.0808 (18); 82.0655 (7)	1
Lycopsamine	R	m	$C_{15}H_{25}NO_5$	300.1805	5.6	94.0654 (100); 156.1018 (55); 138.0912 (35); 120.0807 (18); 82.0656 (7)	1
Rinderine	H	m	$C_{15}H_{25}NO_5$	300.1805	5.9	138.0913 (100); 156.1019 (50); 120.0808 (31); 94.0655 (24); 82.0656 (12)	2
Echinatine	H	m	$C_{15}H_{25}NO_5$	300.1805	6.0	138.0912 (100); 156.1018 (55); 120.0808 (33); 94.0654 (26); 82.0656 (13)	2
Supinine NO	S	-	$C_{15}H_{25}NO_5$	300.1805	8.7	156.1020 (100); 139.0992 (34); 120.0809 (24); 122.0965 (22); 121.0887 (9); 138.0913 (7); 960812 (7)	2
Amabiline NO	S	-	$C_{15}H_{25}NO_5$	300.1805	9.1	156.1019 (100); 139.0991 (32); 120.0808 (26); 122.0965 (26); 121.0887 (10); 138.0913 (8); 960812 (7)	3
Curassavine	T	-	$C_{16}H_{29}NO_4$	300.2169	11.9	142.1227 (100); 124.1122 (75); 156.1022 (12); 70.0658 (12); 96.0812 (10)	2
Dihydroechinatine (rinderine)	P	m	$C_{15}H_{27}NO_5$	302.1962	6.5	158.1176 (100); 140.1069 (56);122.0963 (41); 96.0812 (18)	3
Dihydrointermedine	P	m	$C_{15}H_{27}NO_5$	302.1962	6.6	158.1175 (100); 140.1068 (55); 122.0964 (36); 96.0811 (14)	3
Dihydrolycopsamine	P	m	$C_{15}H_{27}NO_5$	302.1962	6.7	158.1175 (100); 140.1069 (55); 122.0965 (34); 96.0810 (12)	3
Viridiflorine NO	T	-	$C_{15}H_{27}NO_5$	302.1962	8.5	158.1176 (100); 124.1121 (16); 141.1148 (9), 140.1071 (7); 122.0966 (2)	3
Helioamplexine	R	m	$C_{16}H_{27}NO_5$	314.1962	7.4	94.0655 (100); 156.1019 (36); 138.0914 (30); 120.0809 (17); 82.0657 (9)	2
Heliotrine	H	m	$C_{16}H_{27}NO_5$	314.1962	9.2	138.0912 (100); 156.1017 (43); 94.0654 (29); 120.0808 (27); 82.0656 (14); 108.0809 (9)	1
Heleurine NO	S	-	$C_{16}H_{27}NO_5$	314.1962	12.4	156.1019 (100); 120.0808 (20); 139.0991 (18); 122.0965 (16); 138.0914 (8); 121.0889 (5); 96.0811 (3)	2
5'-Hydroxyindicine	R	m	$C_{15}H_{25}NO_6$	316.1755	1.9	94.0654 (100); 138.0912 (43); 156.1017 (25); 120.0808 (18); 82.0656 (5); 108.0809 (2)	2
5'-Hydroxyintermedine (lycopsamine)	R	m	$C_{15}H_{25}NO_6$	316.1755	3.0	94.0654 (100); 138.0912 (40); 156.1018 (26); 120.0808 (16); 82.0655 (5); 108.0809 (2)	3
5'-Hydroxyechinatine (rinderine)	H	m	$C_{15}H_{25}NO_6$	316.1755	3.5	138.0913 (100); 94.0653 (28); 72.0813 (23); 156.1017 (21); 120.0809 (8)	2
Rinderine NO	H	m	$C_{15}H_{25}NO_6$	316.1755	6.4	172.0965 (100); 138.0912 (19); 111.0680 (18); 94.0654 (18); 136.0757 (7); 137.0835 (3); 155.0939 (18)	2
Echinatine NO	H	m	$C_{15}H_{25}NO_6$	316.1755	6.6	172.0965 (100); 138.0912 (20); 111.0680 (20); 94.0654 (19); 136.0757 (7); 137.0833 (3); 155.0939 (16)	2
Intermedine NO	R	m	$C_{15}H_{25}NO_6$	316.1755	6.9	172.0965 (100); 138.0912 (53); 94.0654 (37); 111.068 (25); 155.0938 (18); 136.0756 (15); 137.0836 (6)	1
Indicine NO	R	m	$C_{15}H_{25}NO_6$	316.1755	7.2	172.0964 (100); 138.0912 (53); 94.0654 (37); 111.0679 (23); 136.0754 (18); 137.0833 (7); 155.0938 (1)	1
Lycopsamine NO	R	m	$C_{15}H_{25}NO_6$	316.1755	7.2	172.0966 (100); 138.0912 (64); 94.0654 (41); 111.0681 (24); 136.0758 (19); 155.0939 (18); 137.0834 (6)	1
Dihydrointermedine NO	P	m	$C_{15}H_{27}NO_6$	318.1911	7.6	174.1122 (100); 113.0837 (20); 96.0810 (3); 140.1069 (2); 138.0913 (1); 139.0990 (1)	3
Dihydrolycopsamine NO	P	m	$C_{15}H_{27}NO_6$	318.1911	7.7	174.1122 (100); 113.0837 (20); 96.0811 (3); 140.1070 (2); 138.0912 (1); 139.0990 (1)	3

Dihydrorinderine NO	P	m	$C_{15}H_{27}NO_6$	318.1911	8.0	174.1123 (100); 96.0811 (26); 113.0837 (23); 140.1068 (22); 138.0913 (10); 139.0994 (2)	3
Dihydroechinatine NO	P	m	$C_{15}H_{27}NO_6$	318.1911	8.1	174.1123 (100); 96.0811 (41); 140.1068 (25); 113.0837 (25); 138.0912 (13); 139.0994 (2)	3
Monocrotaline	R	c	$C_{16}H_{23}NO_6$	326.1598	2.7	120.0808 (82); 121.0885 (80); 94.0654 (31); 237.1358 (21); 194.1175 (20); 280.1540 (16); 138.0911 (15); 298.1642 (6)	1
Europine	H	m	$C_{16}H_{27}NO_6$	330.1911	5.9	138.0913 (100); 156.1019 (41); 94.0655 (22); 120.0809 (18); 254.1383 (11); 82.0657 (11); 108.0810 (5)	1
Helioamplexine NO	R	m	$C_{16}H_{27}NO_6$	330.1911	9.2	172.0966 (100); 138.0913 (83); 94.0654 (65); 111.0681 (32); 155.0939 (29); 136.0757 (24); 137.0837 (8)	3
Heliotrine NO	H	m	$C_{16}H_{27}NO_6$	330.1911	10.2	172.0964 (100); 111.0679 (17); 138.0912 (13); 94.0654 (12); 155.0938 (6); 136.0754 (6); 137.0834 (3);	1
5'-Hydroxyechinatine (rinderine) NO	H	m	$C_{15}H_{25}NO_7$	332.1704	1.9	172.0965 (100); 111.0681 (19); 155.0937 (7); 136.0757 (2); 137.0837 (3); 138.0912 (1); 94.0654 (1)	2
5'-Hydroxyintermedine (lycopsamine) NO	R	m	$C_{15}H_{25}NO_7$	332.1704	3.0	172.0965 (100); 138.0912 (30); 94.0654 (24); 111.0680 (19); 155.0938 (16); 136.0757 (11); 137.0835 (5)	2
Spartioidine	R	c	$C_{18}H_{23}NO_5$	334.1649	9.8	120.0807 (67); 94.0654 (41); 138.0912 (35); 306.1696 (21)	2
Seneciphylline	R	c	$C_{18}H_{23}NO_5$	334.1649	10.1	120.0807 (58); 94.0654 (50); 138.0912 (38); 306.1697 (22)	1
Senecivernine	R	c	$C_{18}H_{25}NO_5$	336.1805	12.1	120.0808 (41); 138.0913 (27); 308.1855 (23); 94.0654 (18)	1
Senecionine	R	c	$C_{18}H_{25}NO_5$	336.1805	12.3	120.0808 (51); 94.0654 (45); 138.0912 (33); 308.1851 (19)	1
Monocrotaline NO	R	c	$C_{16}H_{23}NO_7$	342.1547	5.2	137.0833 (76); 119.0729 (39); 120.0808 (33); 136.0755 (24); 118.0651 (23); 236.1278 (19); 94.0654 (19); 296.1491 (8); 138.0913 (7); 314.1587 (4)	1
3'-Acetylintermedine	R	m	$C_{17}H_{27}NO_6$	342.1911	8.8	94.0655 (100); 138.0914 (22); 120.0809 (20); 156.1017 (15); 282.1697 (6)	2
3'-Acetylrinderine	H	m	$C_{17}H_{27}NO_6$	342.1911	8.9	138.0913 (100); 120.0809 (36); 94.0655 (27); 156.1017 (19); 282.1707 (6)	2
7-Acetylrinderine	H	d	$C_{17}H_{27}NO_6$	342.1911	9.6	120.0808 (100); 180.1016 (6); 94.0657 (4); 138.0913 (3);	3
7-Acetylechinatine	H	d	$C_{17}H_{27}NO_6$	342.1911	9.7	120.0808 (100); 138.0913 (6); 198.1123 (5); 94.0653 (3); 282.0629 (2); 180.1021 (2)	3
3'-Acetyllycopsamine	R	m	$C_{17}H_{27}NO_6$	342.1911	9.8	94.0656 (100); 138.0913 (27); 120.0810 (20); 156.1020 (14); 282.1695 (4)	2
3'-Acetylechinatine	H	m	$C_{17}H_{27}NO_6$	342.1911	10.2	138.0912 (100); 120.0809 (28); 94.0654 (26); 156.1018 (14); 282.1696 (3)	2
7-Acetylintermedine	R	d	$C_{17}H_{27}NO_6$	342.1911	10.5	120.0807 (100); 198.1122 (6); 94.0654 (5); 180.1016 (5); 138.0912 (3)	2
7-Acetyllycopsamine	R	d	$C_{17}H_{27}NO_6$	342.1911	10.7	120.0807 (100); 94.0654 (7); 198.1123 (7); 180.1014 (4); 138.0913 (3)	2
Europine NO	H	m	$C_{16}H_{27}NO_7$	346.1860	6.5	172.0965 (100); 111.0680 (16); 155.0939 (12); 256.1175 (12); 138.0912 (10); 94.0655 (10); 136.0754 (5); 137.0834 (2)	1
Erucifoline	R	c	$C_{18}H_{23}NO_6$	350.1598	5.5	120.0808 (67); 138.0911 (39); 94.0653 (33); 322.1643 (5)	1
Riddelliine	R	c	$C_{18}H_{23}NO_6$	350.1598	7.1	120.0807 (62); 94.0654 (48); 138.0912 (42); 322.1644 (23)	2
Spartioidine NO	R	c	$C_{18}H_{23}NO_6$	350.1598	11.0	120.0807 (91); 118.0652 (84); 119.0729 (77); 94.0654 (72); 136.0756 (39); 138.0912 (25); 322.1647 (10); 137.0833 (4)	2
Seneciphylline NO	R	c	$C_{18}H_{23}NO_6$	350.1598	11.2	120.0808 (85); 94.0654 (79); 118.0652 (68); 119.0729 (54); 136.0756 (38); 138.0913 (25); 322.1646 (8); 137.0832 (5)	1
Retrorsine	R	c	$C_{18}H_{25}NO_6$	352.1755	8.8	120.0808 (51); 94.0654 (36); 138.0912 (34); 324.1798 (18)	1
Jacobine	R	c	$C_{18}H_{25}NO_6$	352.1755	10.4	120.0808 (100); 155.1065 (62); 122.0964 (57); 123.1043 (37); 94.0655 (34); 280.1547 (28); 140.1068 (11); 138.0913 (9)	1
Senecivernine NO	R	c	$C_{18}H_{25}NO_6$	352.1755	12.6	120.0807 (57); 118.0652 (54); 94.0654 (53); 119.0731 (35); 136.0757 (21); 138.0912 (15); 324.1804 (9); 137.0838 (3)	1
Integerrimine NO	R	c	$C_{18}H_{25}NO_6$	352.1755	12.7	118.0652 (68); 120.0807 (56); 94.0654 (52); 119.0729 (50); 136.0756 (41); 138.0912 (16); 324.1799 (8); 137.0833 (4)	2
Senecionine NO	R	c	$C_{18}H_{25}NO_6$	352.1755	12.8	118.0651 (55); 120.0808 (50); 94.0654 (50); 136.0756 (43); 119.0730 (37); 138.0913 (17); 324.1799 (6); 137.0836 (5)	1
Trichodesmine	R	c	$C_{18}H_{27}NO_6$	354.1911	8.1	222.1487 (100); 120.0808 (83); 94.0654 (30); 164.1069 (19); 308.1850 (17); 138.0912 (16)	1
Uplandicine	R	d	$C_{17}H_{27}NO_7$	358.1860	6.2	120.0808 (100); 94.0655 (6); 180.1018 (4); 198.1127 (3); 138.0915 (2)	2
3'-Acetylrinderine NO	H	m	$C_{17}H_{27}NO_7$	358.1860	9.9	172.0966 (100); 298.1646 (37); 138.0912 (28); 94.0655 (26); 111.0681 (26); 155.0939 (18); 136.0756 (11); 137.0834 (4)	2

7-Acetylintermedine NO	R	d	$C_{17}H_{27}NO_7$	358.1860	10.7	214.1070 (100); 137.0834 (50); 180.1016 (43); 136.0756 (24); 120.0808 (22); 119.0731 (19); 118.0651 (14)	2
3'-Acetylintermedine NO	R	m	$C_{17}H_{27}NO_7$	358.1860	10.8	172.0967 (100); 138.0913 (73); 94.0655 (61); 298.1649 (54); 111.0682 (33); 136.0757 (23); 155.0939 (21); 137.0837 (8)	3
3'-Acetylechinatine NO	H	m	$C_{17}H_{27}NO_7$	358.1860	10.9	172.0965 (100); 138.0912 (37); 298.1647 (35); 94.0654 (33); 111.0680 (23); 155.0938 (17); 136.0756 (16); 137.0833 (4)	3
7-Acetyllycopsamine NO	R	d	$C_{17}H_{27}NO_7$	358.1860	11.0	214.1071 (100); 180.1015 (53); 137.0835 (51); 136.0757 (25); 120.0807 (23); 119.0732 (16); 118.0652 (14)	2
7-Acetylrinderine NO	H	d	$C_{17}H_{27}NO_7$	358.1860	11.3	214.1070 (100); 137.0835 (81); 119.0730 (75); 120.0807 (62); 136.0756 (28); 118.0650 (25); 180.1019 (10); 298.1652 (5); 138.0911 (5);	3
7-Acetylechinatine NO	H	d	$C_{17}H_{27}NO_7$	358.1860	11.4	214.1072 (100); 137.0835 (76); 120.0808 (62); 119.0731 (60); 106.0654 (50); 136.0757 (25); 118.0653 (22); 298.1662 (3); 138.0915 (6)	3
3'-Acetyllycopsamine NO	R	m	$C_{17}H_{27}NO_7$	358.1860	11.7	172.0968 (100); 138.0914 (87); 94.0656 (77); 298.1648 (53); 111.0682 (33); 136.0758 (29); 155.0939 (17); 137.0837 (9)	2
Erucifoline NO	R	c	$C_{18}H_{23}NO_7$	366.1547	6.2	118.0651 (93); 119.0730 (86); 94.0654 (80); 120.0808 (78); 136.0755 (68); 137.0835 (9); 138.0913 (10)	1
Riddelliine NO	R	c	$C_{18}H_{23}NO_7$	366.1547	7.7	120.0808 (100); 94.0654 (99); 118.0652 (78); 119.0730 (70); 136.0757 (51); 138.0913 (26); 338.1598 (7); 137.0832 (6)	2
Neosenkirkine	O	c	$C_{19}H_{27}NO_6$	366.1911	12.9	168.1021 (100); 150.0915 (52); 122.0603 (25)	2
Senkirkine	O	c	$C_{19}H_{27}NO_6$	366.1911	13.3	168.1018 (100); 150.0911 (34); 122.0600 (34); 348.1821 (2)	1
Jacobine NO	R	c	$C_{18}H_{25}NO_7$	368.1704	7.3	120.0808 (100); 296.1488 (62); 94.0654 (28); 118.0651 (25); 119.0729 (22); 139.0992 (10); 138.0914 (8)	1
Retrorsine NO	R	c	$C_{18}H_{25}NO_7$	368.1704	9.4	120.0808 (68); 118.0652 (67); 94.0654 (67); 136.0757 (53); 119.0731 (43); 138.0912 (24); 340.1743 (7); 137.0835 (7)	1
Uplandicine NO	R	d	$C_{17}H_{27}NO_8$	374.1809	6.2	214.1070 (100); 137.0835 (35); 180.1015 (19); 136.0756 (16); 120.0807 (15); 119.0731 (9); 118.0651 (6)	2
Acetylseneciphylline NO	R	c	$C_{20}H_{25}NO_6$	376.1755	16.0	118.0653 (100); 120.0809 (94); 94.0655 (76); 119.0731 (57); 136.0758 (47); 332.1490 (21); 138.0915 (16); 137.0594 (2)	2
Symphytine isomer 1	R	d	$C_{20}H_{31}NO_6$	382.2224	15.4	120.0808 (100); 83.0496 (22); 238.1436 (6); 138.0914 (4); 94.0654 (2)	2
Symphytine isomer 2	R	d	$C_{20}H_{31}NO_6$	382.2224	15.6	120.0808 (100); 83.0496 (61); 138.0914 (8); 238.1432 (8); 94.0655 (4); 220.1331 (1)	2
Echiumine	R	d	$C_{20}H_{31}NO_6$	382.2224	15.7	120.0807 (100); 138.0912 (41); 94.0654 (15); 83.0496 (5); 220.1332 (5); 238.1439 (2)	2
5'-Acetyleuropine NO	H	m	$C_{18}H_{29}NO_8$	388.1966	11.3	172.0965 (100); 137.0834 (58); 328.1749 (38); 111.0679 (11); 138.0911 (11); 136.0753 (5)	2
7-Angeloylheliotrine	H	d	$C_{21}H_{33}NO_6$	396.2381	16.4	120.0809 (100); 138.0913 (6); 94.0654 (3)	3
Asperumine	H	d	$C_{20}H_{31}NO_7$	398.2173	13.1	120.0809 (100); 138.0913 (6); 94.0653 (3); 238.1425 (2); 83.0495 (1)	2
Echimidine isomer 1	R	d	$C_{20}H_{31}NO_7$	398.2173	13.2	120.0808 (100); 83.0497 (15); 238.1438 (2); 138.0916 (2); 94.0656 (2); 220.1332 (1)	3
Heliosupine	H	d	$C_{20}H_{31}NO_7$	398.2173	13.3	120.0809 (100); 138.0915 (4); 238.1434 (2); 220.1333 (2); 94.0654 (2); 83.0496 (2)	2
Echimidine isomer 2	R	d	$C_{20}H_{31}NO_7$	398.2173	13.4	120.0808 (100); 83.0495 (63); 138.0913 (5); 238.1424 (3); 94.0654 (3);	3
Echimidine	R	d	$C_{20}H_{31}NO_7$	398.2173	13.4	120.0808 (100); 83.0496 (20); 238.1431 (2); 138.0913 (2); 94.0656 (2);	1
Symphytine NO	R	d	$C_{20}H_{31}NO_7$	398.2173	15.5	254.1383 (100); 83.0496 (86); 137.0834 (53); 220.1330 (49); 120.0807 (39); 136.0758 (36); 119.0729 (27); 118.0652 (23)	2
Echiumine NO	R	d	$C_{20}H_{31}NO_7$	398.2173	15.7	83.0496 (100); 254.1385 (75); 137.0834 (40); 220.1329 (38); 136.0757 (37); 120.0809 (29);119.0730 (17); 118.0651 (15); 138.0913 (6)	2
Canescine (canescenine)	H	d	$C_{20}H_{33}NO_7$	400.2330	12.4	120.0809 (100); 94.0655 (9); 138.0914 (5); 256.1535 (3); 83.0496 (1)	3
7-Tigloyleuropine	H	d	$C_{21}H_{33}NO_7$	412.2330	14.9	120.0809 (100); 138.0915 (4); 94.0655 (3); 238.1434 (2); 220.1334 (1); 83.0495 (1)	2
Lasiocarpine	H	d	$C_{21}H_{33}NO_7$	412.2330	15.1	120.0807 (100); 138.0911 (5); 94.0654 (4); 238.1437 (3); 220.1321 (2); 83.0495 (1)	1
7-Angeloylheliotrine NO	H	d	$C_{21}H_{33}NO_7$	412.2330	16.7	120.0809 (100); 94.0655 (87); 138.0912 (52); 254.138 (51); 119.0731 (48); 136.0757 (47); 137.0836 (30); 118.0653 (25)	2

Echihumiline NO	R	d	$C_{20}H_{31}NO_8$	414.2122	13.2	254.1387 (100); 137.0836 (44); 83.0496 (44);120.0808 (26); 136.0757 (23); 220.1331 (16); 119.0732 (13); 118.0655 (11)	3
Echimidine NO	R	d	$C_{20}H_{31}NO_8$	414.2122	13.4	254.1384 (100); 83.0496 (40); 137.0834 (34); 120.0807 (32); 136.0756 (21); 220.1331 (20); 119.0730 (17); 118.0653 (8); 138.0913 (3)	1
Vulgarine NO	R	m	$C_{20}H_{31}NO_8$	414.2122	13.5	172.0967 (100); 256.1178 (49); 94.0656 (43); 138.0914 (42); 136.0757 (27); 111.0682 (17); 155.0938 (11)	3
Asperumine NO	H	d	$C_{20}H_{31}NO_8$	414.2122	13.7	119.0731 (100); 120.0809 (76); 137.0836 (74); 94.0655 (64); 254.1384 (59); 136.0757 (56); 138.0913 (35); 121.0889 (34); 118.0652 (34)	3
Heliosupine NO	H	d	$C_{20}H_{31}NO_8$	414.2122	14.1	94.0655 (100); 119.0731 (81); 137.0836 (81); 120.0809 (80); 254.1384 (75); 138.0915 (76); 136.0758 (74); 118.0652 (30)	2
Lithosenine	R	d	$C_{20}H_{33}NO_8$	416.2279	8.3	120.0807 (100); 94.0654 (8); 138.0913 (4); 256.1540 (1)	3
Canescine (canescenine) NO	H	d	$C_{20}H_{33}NO_8$	416.2279	12.7	272.1491 (90); 137.0835 (58); 136.0757 (41); 120.0809 (33); 119.0730 (23); 118.0651 (23); 138.0913 (21)	3
7-Tigloyleuropine NO	H	d	$C_{21}H_{33}NO_8$	428.2279	15.6	119.0730 (100); 120.0808 (95); 254.1381 (83); 137.0834 (81); 136.0756 (65); 118.0651 (32); 138.0913 (33)	2
Lasiocarpine NO	H	d	$C_{21}H_{33}NO_8$	428.2279	15.8	94.0654 (100); 254.1384 (91); 120.0808 (90); 119.0731 (83); 136.0757 (77); 137.0835 (76); 138.0913 (72); 118.0652 (60)	1
Lithosenine NO	R	d	$C_{20}H_{33}NO_9$	432.2228	8.7	272.1490 (100); 137.0835 (46); 120.0809 (26); 136.0757 (25); 119.0731 (18); 138.0916 (14); 118.0652 (11)	3
Thesinine-4'-ramnoside	T	-	$C_{23}H_{31}NO_7$	434.2173	13.6	147.0440 (100); 142.1227 (26); 124.1121 (25); 119.0493 (17); 288.1594 (15)	3
3'-Acetylheliosupine	H	d	$C_{22}H_{33}NO_8$	440.2279	15.0	120.0809 (100); 138.0913 (4); 238.1438 (2); 83.0495 (2); 220.1335 (1)	2
3'-Acetylechiumine NO	R	d	$C_{22}H_{33}NO_8$	440.2279	16.7	83.0496 (100); 254.1387 (40); 380.2062 (34); 220.1331 (34); 136.0755 (32); 137.0835 (30); 120.0809 (30); 118.0652 (18); 119.0730 (15)	3
Thesinine-4'-glucoside	T	-	$C_{23}H_{31}NO_8$	450.2122	11.1	147.0440 (100); 142.1222 (20); 124.1122 (20); 119.0493 (17); 288.1591 (6)	3
5'-Acetyllasiocarpine	H	d	$C_{23}H_{35}NO_8$	454.2435	16.4	120.0808 (100); 138.0912 (7); 238.1439 (6); 94.0654 (3); 220.1333 (2); 83.0495 (2)	2
3'-Acetylheliosupine NO	H	d	$C_{22}H_{33}NO_9$	456.2228	15.6	94.0655 (100); 119.0731 (95); 138.0913 (83); 120.0808 (61); 136.0759 (55); 254.1386 (52); 137.0836 (38); 118.0652 (35); 396.2015 (3)	2
5'-Acetyllasiocarpine NO	H	d	$C_{23}H_{35}NO_9$	470.2385	16.7	94.0655 (100); 120.0809 (87); 254.1382 (75); 138.0914 (73); 136.0757 (65); 119.0731 (63); 137.0834 (58); 118.0650 (30); 410.2153 (25)	2

690 [a] NO, N-oxide; [b] R, retronecine; H, heliotridine; O, otonecine; T, trachelanthamidine; P, platynecine; S, supinidine; [c] m, monoester; d, open-chained
691 diester; c, cyclic diester; [d] exact mass; [e] IL, identification level according to Metabolomics Standards Initiative.

692

693 **Table 2.** Extraction efficiencies (EEs) and Limits of identification (LOIs) of the 28 target PAs in different food matrices.

Compound	Honey		Pollen		Black tea		Green tea		Herbal infusion		Dietary supplement	
	EE (SD)	LOI (µg kg^{-1})	EE (SD)	LOI (µg kg^{-1})	EE (SD)	LOI (µg kg^{-1})	EE (SD)	LOI (µg kg^{-1})	EE (SD)	LOI (µg kg^{-1})	EE (SD)	LOI (µg kg^{-1})
Echimidine	80.1 (2.8)	0.6	94.8 (0.4)	10.4	89.6 (3.2)	3.0	94.9 (8.9)	3.2	83.5 (8.2)	3.0	95.5 (1.6)	20.0
Echimidine NO	98.7 (2.4)	0.6	100.3 (2.8)	10.4	109.1 (5.0)	3.0	94.0 (7.2)	9.4	106.0 (6.5)	3.0	105.5 (0.6)	20.0
Erucifoline	94.3 (7.8)	0.6	95.6 (8.3)	15.6	88.8 (5.3)	7.5	89.6 (7.6)	11.7	93.5 (6.2)	3.0	101.7 (5.5)	20.0
Erucifoline NO	92.9 (4.4)	0.6	87.2 (7.2)	10.4	89.8 (7.1)	4.5	91.3 (2.4)	9.4	94.3 (5.9)	3.0	85.1 (2.3)	10.0
Europine	96.4 (4.9)	1.3	97.7 (5.7)	15.6	96.5 (5.6)	9.4	92.1 (2.7)	9.4	90.4 (3.2)	9.4	91.1 (4.4)	10.0
Europine NO	71.4 (4.5)	0.6	81.4 (9.1)	15.6	72.6 (5.6)	6.0	75.9 (5.8)	9.4	73.1 (6.9)	7.5	70.8 (3.2)	10.0
Heliotrine	87.1 (6.3)	0.6	98.5 (4.0)	4.2	91.5 (6.3)	3.0	90.9 (5.2)	4.7	96.1 (7.1)	3.0	93.8 (2.6)	10.0
Heliotrine NO	90.9 (3.0)	0.6	84.2 (1.0)	12.5	88.6 (4.9)	7.5	88.0 (6.1)	7.8	87.2 (5.7)	3.0	86.4 (0.6)	10.0
Intermedine	91.2 (1.6)	0.6	90.6 (1.5)	8.3	93.3 (0.9)	4.5	95.4 (3.7)	9.4	88.9 (0.9)	3.0	89.8 (6.9)	10.0
Intermedine NO	75.3 (0.8)	0.6	78.3 (3.7)	8.3	73.1 (3.7)	6.0	80.4 (4.3)	9.4	76.5 (1.4)	3.0	70.8 (2.6)	10.0
Jacobine	91.8 (8.0)	0.8	94.3 (11.1)	15.6	95.2 (3.9)	9.4	85.9 (9.1)	11.7	89.7 (7.1)	3.0	104.5 (6.0)	20.0
Jacobine NO	86.1 (5.6)	0.6	95.4 (6.2)	12.5	87.6 (5.9)	4.5	89.7 (3.9)	7.8	92.8 (2.4)	3.0	88.2 (1.6)	10.0
Lasiocarpine	89.8 (2.7)	0.6	99.2 (5.1)	10.4	100.2 (5.1)	3.0	99.1 (7.1)	4.7	95.7 (5.7)	3.0	96.9 (5.9)	10.0
Lasiocarpine NO	90.5 (0.8)	0.6	89.8 (4.6)	12.5	95.0 (4.3)	4.5	93.8 (2.3)	15.0	92.0 (6.2)	3.0	97.4 (4.0)	10.0
Lycopsamine	91.1 (0.4)	0.6	92 (2.1)	4.2	93.5 (1.6)	3.0	91.6 (2.4)	3.2	87.3 (0.5)	3.0	91.9 (4.0)	10.0
Lycopsamine NO	69.7 (5.7)	0.6	73.6 (0.7)	4.2	68.8 (4.5)	3.0	69.3 (5.8)	3.2	72.4 (5.3)	3.0	70.2 (6.1)	10.0
Monocrotaline	94.2 (4.9)	1.3	89.9 (8.4)	15.6	91.2 (3.0)	6.0	93.3 (6.1)	11.7	90.8 (7.1)	4.5	98.7 (5.5)	20.0
Monocrotaline NO	74.9 (5.7)	1.3	76.7 (0.9)	15.6	75.3 (6.9)	7.5	77.4 (5.3)	9.4	77.0 (5.4)	4.5	79.6 (6.9)	10.0
Retrorsine	100.7 (2.5)	0.6	80.0 (3.3)	15.6	98.8 (3.3)	4.5	104.2 (13.2)	6.2	74.1 (7.9)	4.5	99.2 (1.2)	20.0
Retrorsine NO	83.2 (3.1)	0.6	108.3 (5.2)	30.0	106.2 (3.2)	15.0	90.2 (8.6)	11.7	112.9 (4.0)	9.4	95.9 (1.6)	20.0
Senecionine	77.8 (2.6)	0.6	90.7 (9.3)	15.6	88.8 (3.3)	6.0	96.4 (5.7)	11.7	102.3 (5.4)	3.0	99.5 (2.6)	10.0
Senecionine NO	101.8 (3.4)	0.6	99.5 (6.8)	20.0	101.1 (2.8)	3.0	87.1 (5.8)	11.7	102.4 (4.2)	3.0	93.6 (1.0)	10.0
Seneciphylline	84.9 (3.6)	0.6	89.5 (7.1)	15.6	93.3 (0.8)	3.0	89.1 (4.8)	9.4	88.9 (0.9)	3.0	102.4 (3.9)	10.0
Seneciphylline NO	91.9 (6.4)	0.6	101.4 (4.0)	10.4	88.8 (4.1)	4.5	89.6 (4.6)	9.4	93.5 (6.2)	3.0	91.5 (0.5)	20.0
Senecivernine	81.3 (0.0)	0.6	86.0 (9.1)	20.0	91.6 (5.0)	9.4	88.3 (5.3)	7.8	93.4 (4.3)	3.0	100.9 (6.4)	20.0
Senecivernine NO	94.3 (5.6)	0.6	90.9 (8.4)	4.2	96.9 (3.1)	3.0	96.0 (3.7)	7.8	91.5 (6.4)	3.0	92.8 (0.9)	20.0
Senkirkine	99.2 (8.7)	0.6	102.6 (0.6)	4.2	96.8 (8.7)	3.0	97.2 (7.9)	3.2	94.3 (3.9)	3.0	98.1 (5.2)	10.0
Trichodesmine	95.2 (8.2)	1.3	97.3 (0.2)	15.6	90.5 (5.0)	4.5	92.3 (7.1)	7.8	88.2 (3.2)	3.0	96.2 (3.1)	10.0

694 [a] NO: N-oxide

Highlights:

- An analytical platform for the detection of PAs/PANOs in food matrices
- A diagnostic product ions filtering strategy for the characterization of PAs/PANOs
- An internal database of 779 known and expected unknown PAs/PANOs
- A spectral library containing HRMS/MS information of 118 PAs/PANOs
- The platform offers the possibility to detect both target and untarget PAs/PANOs

Fig. 1

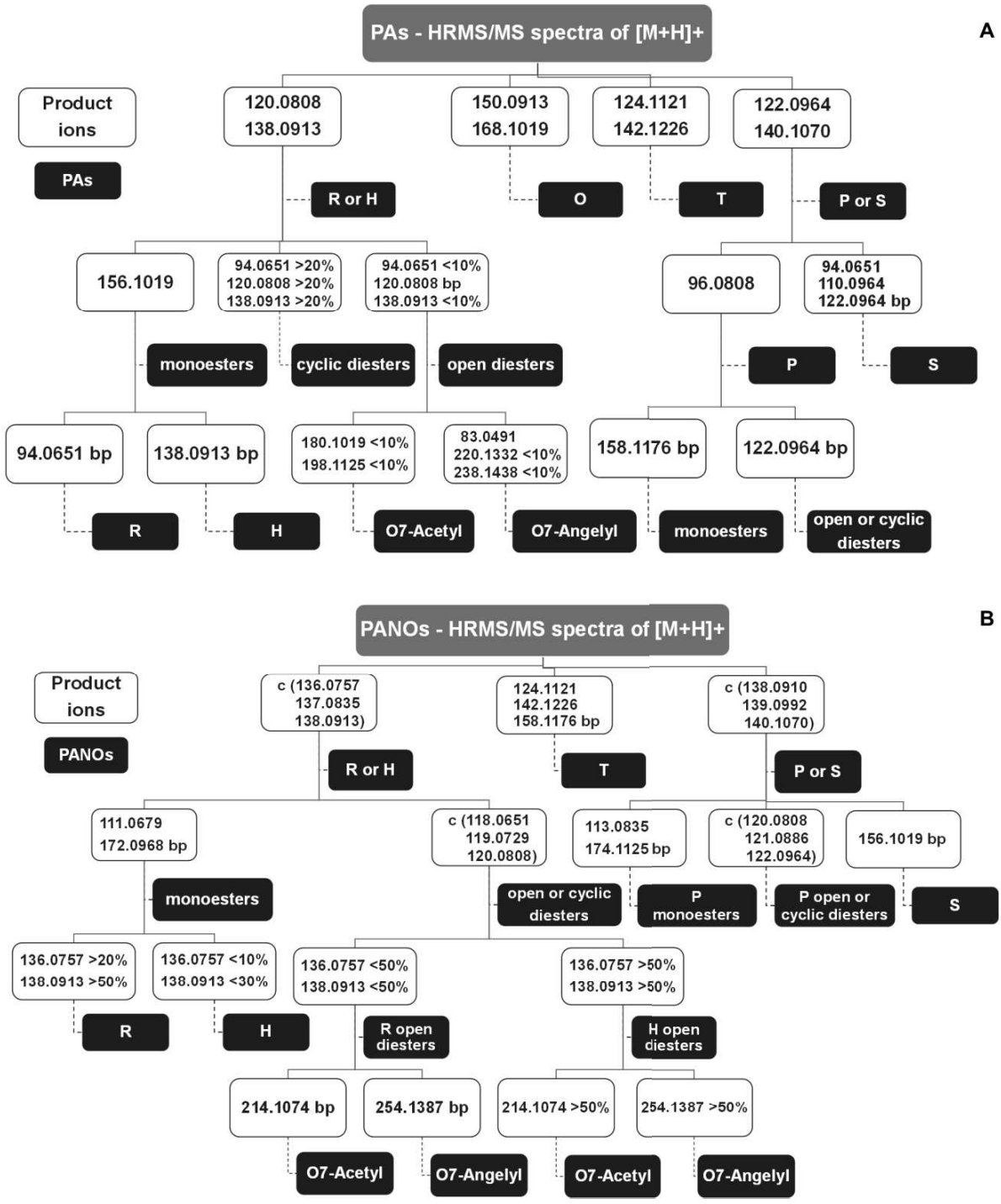

Fig. 2

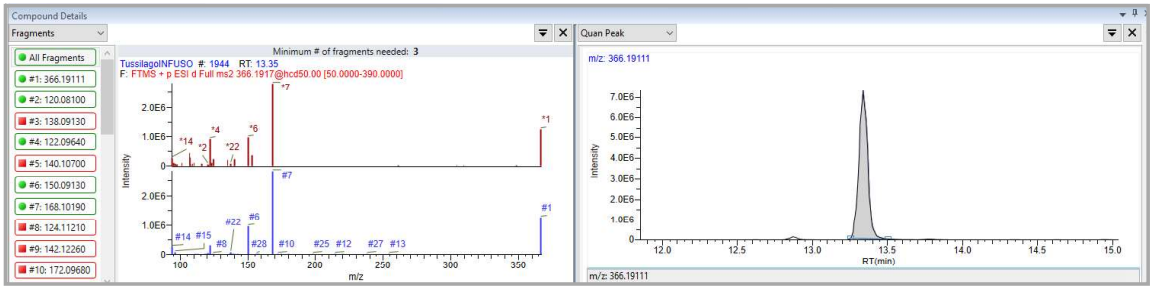

A

Flowchart: Otonecine type PA

Name	Expected Unknowns	CAS Registry Number	Molecular formula[b]	Molecular Weight	[M+H]+ (calculated m	Necine base type[c]	Necic acid type	N-oxide	Isomer group	Isomer subgroup
Crotaverrine		60827-69-2	**C19H27NO6**	365.1833	366.1911	otonecine	cyclic diester		47	A
Emiline		36506-99-7	C19H27NO6	365.1833	366.1911	otonecine	cyclic diester		47	A
Neosenkirkine		57194-70-4	C19H27NO6	365.1833	366.1911	otonecine	cyclic diester		47	A
Senkirkine		2318-18-5	C19H27NO6	365.1833	366.1911	otonecine	cyclic diester		47	A

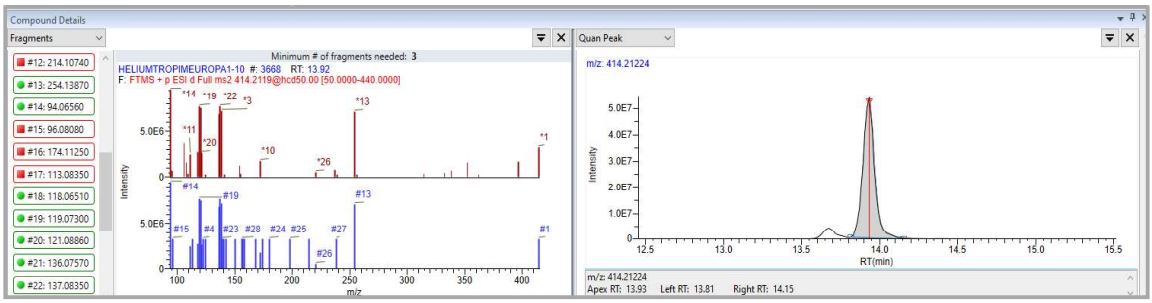

B

Flowchart: Heliotridine open-chained diester type PANO

Name	Expected Unknowns	CAS Registry Number	Molecular formula[b]	Molecular Weight	[M+H]+ (calculated m	Necine base type[c]	Necic acid type	N-oxide	Isomer group	Isomer subgroup
2'-epi-Heliosupine N-oxide		2171456-54-3	C20H31NO8	413.2044	414.2122	heliotridine	open chained diester	X	81	D
Asperumine N-oxide		54324-54-8	C20H31NO8	413.2044	414.2122	heliotridine	open chained diester	X	81	D
Heliosupine N-oxide (Cynoglossophine N-oxide)		31701-88-9	C20H31NO8	413.2044	414.2122	heliotridine	open chained diester	X	81	D

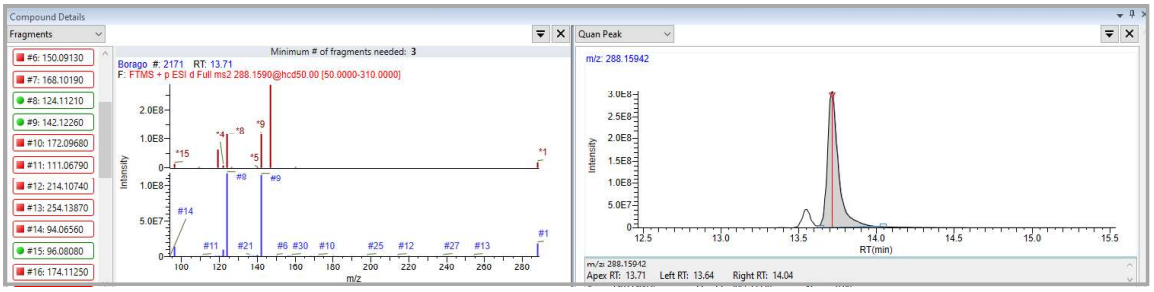

C

Flowchart: Trachelanthamidine type PA

Name	Expected Unknowns	CAS Registry Number	Molecular formula[b]	Molecular Weight	[M+H]+ (calculated m	Necine base type[c]	Necic acid type	N-oxide	Isomer group	Isomer subgroup
Thesinine		488-02-8	**C17H21NO3**	287.1516	288.1594	trachelanthamidine	-		9	A

Fig. 3.

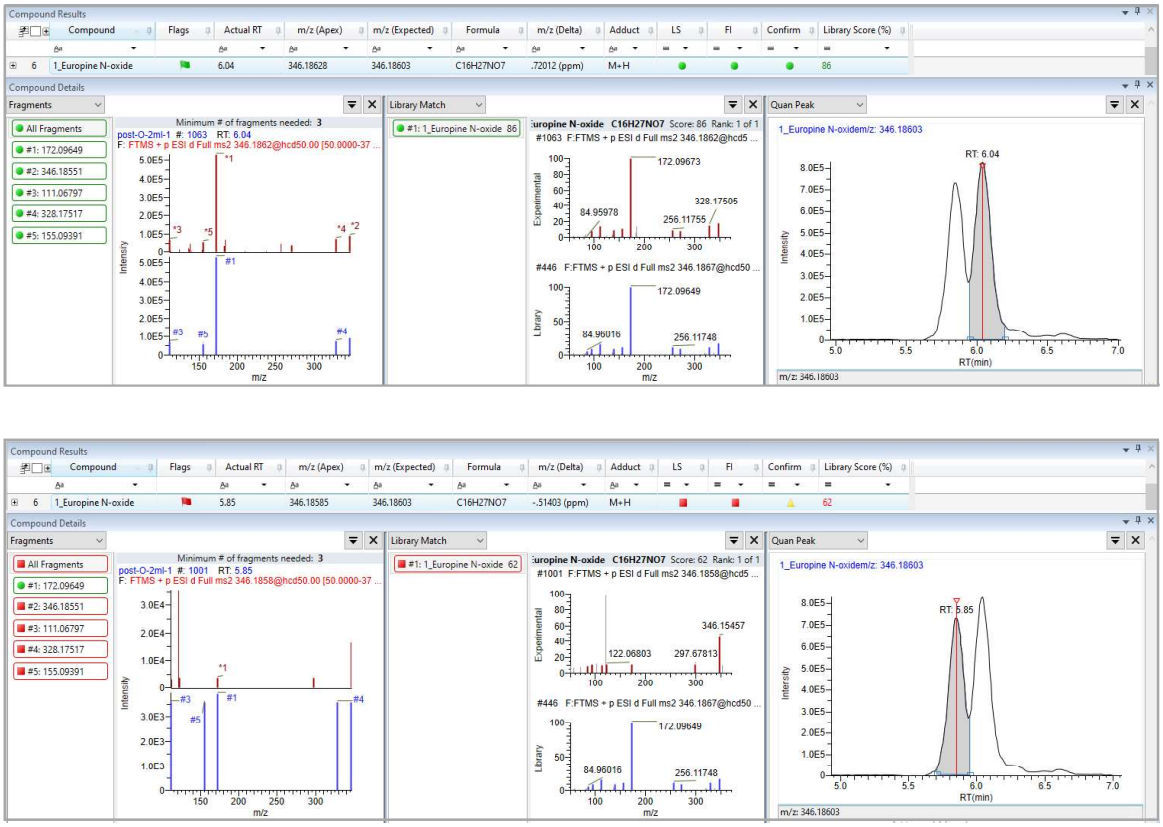

Fig. 4.